Polymer 52 (2011) 5–25

Contents lists available at ScienceDirect

Polymer

journal homepage: www.elsevier.com/locate/polymer

Feature Article

Graphene-based polymer nanocomposites

Jeffrey R. Potts [a], Daniel R. Dreyer [b], Christopher W. Bielawski [b,*], Rodney S. Ruoff [a,**]

[a] Department of Mechanical Engineering and the Texas Materials Institute, The University of Texas at Austin, 204 E. Dean Keeton St., Austin, TX 78712, USA
[b] Department of Chemistry and Biochemistry, The University of Texas at Austin, One University Station A5300, Austin, TX 78712, USA

ARTICLE INFO

Article history:
Received 15 September 2010
Received in revised form
22 November 2010
Accepted 24 November 2010
Available online 2 December 2010

Keywords:
Graphene
Polymer nanocomposites
Nanotechnology

ABSTRACT

Graphene-based materials are single- or few-layer platelets that can be produced in bulk quantities by chemical methods. Herein, we present a survey of the literature on polymer nanocomposites with graphene-based fillers including recent work using graphite nanoplatelet fillers. A variety of routes used to produce graphene-based materials are reviewed, along with methods for dispersing these materials in various polymer matrices. We also review the rheological, electrical, mechanical, thermal, and barrier properties of these composites, and how each of these composite properties is dependent upon the intrinsic properties of graphene-based materials and their state of dispersion in the matrix. An overview of potential applications for these composites and current challenges in the field are provided for perspective and to potentially guide future progress on the development of these promising materials.

1. Introduction

Graphene, a monolayer of sp^2-hybridized carbon atoms arranged in a two-dimensional lattice, has attracted tremendous attention in recent years owing to its exceptional thermal, mechanical, and electrical properties [1–3]. One of the most promising applications of this material is in polymer nanocomposites, polymer matrix composites which incorporate nanoscale filler materials. Nanocomposites with exfoliated layered silicate fillers have been investigated as early as 1950 [4], but significant academic and industrial interest in nanocomposites came nearly forty years later following a report from researchers at Toyota Motor Corporation that demonstrated large mechanical property enhancement using montmorillonite as filler in a Nylon-6 matrix [5]. Polymer nanocomposites show substantial property enhancements at much lower loadings than polymer composites with conventional micron-scale fillers (such as glass or carbon fibers), which ultimately results in lower component weight and can simplify processing [6]; moreover, the multifunctional property enhancements made possible with nanocomposites may create new applications of polymers [7].

On account of the recent emergence of using graphite oxide (GO) to prepare graphene-based materials for composites and other applications [8], this review will focus primarily on polymer nanocomposites utilizing GO-derived materials as fillers. Emphasis will be directed toward structure–property relationships as well as trends in property enhancements of these composites, and comparisons to other nanofillers will be made where appropriate. Some highlights from the literature on polymer composites with what have been referred to as graphite nanoplatelet (GNP) fillers, typically derived from graphite intercalation compounds (GICs), will also be presented and used to provide additional context. Although a review on GO-derived polymer nanocomposites has recently appeared [9], our review considers work with GNP fillers, and provides a historical perspective with more emphasis on preparative methods and processing.

2. Properties and production of graphene-based materials for composite filler

2.1. Overview and history of graphene-based materials

Graphene has a rich history which spans over forty years of experimental work [10]. 'Pristine' graphene (a single, purely sp^2-hybridized carbon layer free of heteroatomic defects) has been produced by several routes [1,11], including growth by chemical vapor deposition (both of discrete monolayers onto a substrate and agglomerated powders), micro-mechanical exfoliation of graphite, and growth on crystalline silicon carbide. While these approaches can yield a largely defect-free material with exceptional physical properties, current techniques of making powdered samples of graphene do not yield large enough quantities for use as composite filler [12].

* Corresponding author. Tel.: +1 512 232 3839; fax: +1 512 471 5884.
** Corresponding author. Tel.: +1 512 471 7681; fax: +1 512 471 4691.
E-mail addresses: bielawski@cm.utexas.edu (C.W. Bielawski), r.ruoff@mail.utexas.edu (R.S. Ruoff).

0032-3861/$ – see front matter © 2010 Elsevier Ltd. All rights reserved.
doi:10.1016/j.polymer.2010.11.042

Scalable approaches to GNPs and graphene-based materials (few-layer platelets or monolayer carbon sheets with heteroatoms and topological defects) primarily utilize GICs or GO as the precursor material, respectively. GO and GICs have been investigated as far back as the 1840s [13,14]. In the 1960s, Boehm and co-workers reported the reduction of dispersions of GO using a variety of chemical reductants [15,16], as well as thermal expansion and reduction [17], producing thin, lamellar carbon containing only small amounts of hydrogen and oxygen. By using transmission electron microscopy (TEM), the carbon material produced by chemical reduction was found to consist of "single carbon layers" [15]. The procedures currently used to produce these graphene-like materials have changed little since this early work [18,19]. Techniques for the exfoliation of GICs have also been developed, although most of these approaches do not yield single-layer sheets but rather platelets with thicknesses typically above approximately 5 nm. Liquid-phase exfoliation of graphite and chemical synthesis of graphene from polycyclic aromatic hydrocarbon precursors may also eventually provide scalable alternative routes for production of graphene [19], as could the further development of gas phase CVD methods [12]. Recently, graphene nanoribbons, produced by "unzipping" of multiwalled carbon nanotubes, have been investigated as composite filler [20].

A variety of uses have been envisioned or demonstrated for GNPs and graphene-based materials, and their use as a composite filler has attracted considerable interest [1]. While polymer nanocomposites incorporating GNP fillers continue to be a significant research focus, recent work has largely focused on use of graphene-based filler materials derived from GO. As will be described in the following sections, GO-derived fillers can exhibit high electrical conductivities (on the order of thousands of S/m) [8], high moduli (reported values ranging from 208 GPa [21] to over 650 GPa [22]), and can be easily functionalized to tailor their compatibility with the host polymer. The reported values of stiffness and electrical conductivity of GO-derived filler materials can be higher than those reported for nanoclays [23], but generally lower than those reported for single-walled carbon nanotubes (SWNTs) [24]. However, the intrinsic mechanical properties and electrical and thermal conductivities of SWNTs may be comparable to those of pristine graphene [24,25]. Moreover, the two-dimensional platelet geometry of graphene and graphene-based materials may offer certain property improvements that SWNTs cannot provide when dispersed in a polymer composite, such as improved gas permeation resistance of the composite [26].

2.2. Exfoliation of graphite

Most exfoliated graphite fillers are derived from GICs, which are compounds of graphite with atoms or molecules (such as alkali metals or mineral acids) intercalated between the carbon layers [27]. The intercalation of graphite increases its interlayer spacing, weakening the interlayer interactions and facilitating the exfoliation of the GIC by mechanical or thermal methods [28]. Varying structural arrangements of the intercalant are possible, such as alternating layers of graphene and intercalant (referred to as first-stage GICs), as well as multiple (two to five) adjacent graphene layers between intercalant layers (higher-stage GICs) [27]. It is the former arrangement, however, which is preferred for the complete exfoliation of these materials into monolayer platelets [29].

Intercalation of graphite by a mixture of sulfuric and nitric acid produces a higher-stage GIC that can be exfoliated by rapid heating or microwave treatment of the dried down powder, producing a material commonly referred to as expanded graphite (EG) [30]. EG retains a layered structure but has slightly increased interlayer spacing relative to graphite, consisting of thin platelets (30–80 nm) which are loosely stacked [30]. Notably, an acid treatment may also oxidize the platelets, albeit to a far lesser degree than GO [31]. EG itself has been investigated as a composite filler [32–34], although its effectiveness in enhancing properties compared with GO-derived fillers is limited by its layered structure and relatively low specific surface area (generally less than 40 m^2/g [35]). To produce a higher surface area material, EG can be further exfoliated by various techniques to yield GNPs down to 5 nm thickness [28,30].

The thickness and lateral dimensions of GNPs vary widely depending on the production method used, and several approaches have been reported. Sonication of EG in appropriate media can yield platelets with thicknesses of roughly 10 nm and with lateral dimensions as large as 15 μm [36]. Smaller platelet thicknesses have been reported by re-intercalation of EG or co-intercalation of GICs with organic molecules prior to exfoliation. For instance, mixing potassium with EG yielded a stoichiometric first-stage GIC (KC_8), which was reported to be exfoliated into GNPs with thicknesses as low as 2 nm upon reaction with water or alcohols, along with sonication [29]. It has also been reported that sulfuric acid-intercalated EG can be co-intercalated with tetrabutylammonium hydroxide (among many other molecules [37]). By sonicating this GIC in *N*,*N*-dimethylformamide (DMF) in the presence of a surfactant (a poly(ethylene glycol)-modified phospholipid), monolayer graphene-like sheets were obtained [31].

The isolation of pristine graphene by micro-mechanical exfoliation [38] has helped to motivate research towards a scalable procedure for liquid-phase exfoliation of graphite to afford high-quality graphene without the use of intercalants; as a result, several different approaches have now been reported [39–42]. Sonication of graphite flakes in water, for example, was reported to yield a mixture of monolayer and multi-layer graphene which was largely defect-free, but this approach required the use of surfactants which may negatively affect the electrical conductivity [41]. Direct exfoliation of graphite into solvents such as propylene carbonate (PC) or *N*-methylpyrrolidone (NMP) [40], and electrochemical exfoliation of graphite in ionic liquids [42] may eventually offer viable alternatives for production of solution-based graphene, although graphene made by these approaches has yet to be studied as composite filler.

2.3. Production and properties of GO

GO is generally produced by the treatment of graphite using strong mineral acids and oxidizing agents, typically via treatment with $KMnO_4$ and H_2SO_4, as in the Hummers method or its modified derivatives, or $KClO_3$ (or $NaClO_3$) and HNO_3 as in the Staudenmaier or Brodie methods [8]. These reactions achieve similar levels of oxidation (C:O ratios of approximately 2:1) [8] which ultimately disrupts the delocalized electronic structure of graphite and imparts a variety of oxygen-based chemical functionalities to the surface. While the precise structure of GO remains a matter of debate [8], it is thought that hydroxyl and epoxy groups are present in highest concentration on the basal plane, with carboxylic acid groups around the periphery of the sheets as shown in Fig. 1. GO has an expanded interlayer spacing relative to graphite which depends on humidity (for instance, 0.6 nm when subjected to high vacuum [43] to roughly 0.8 nm at 45% relative humidity [44]) due to intercalation of water molecules [43]. GO can be exfoliated using a variety of methods (most commonly by thermal shocking [45] or chemical reduction in appropriate media [11,46]), yielding a material reported to be structurally similar to that of pristine graphene on a local scale; these techniques will be discussed in more detail below.

2.4. Exfoliation of GO

With a few exceptions, production of well-dispersed polymer nanocomposites with GO-derived fillers hinges largely on the

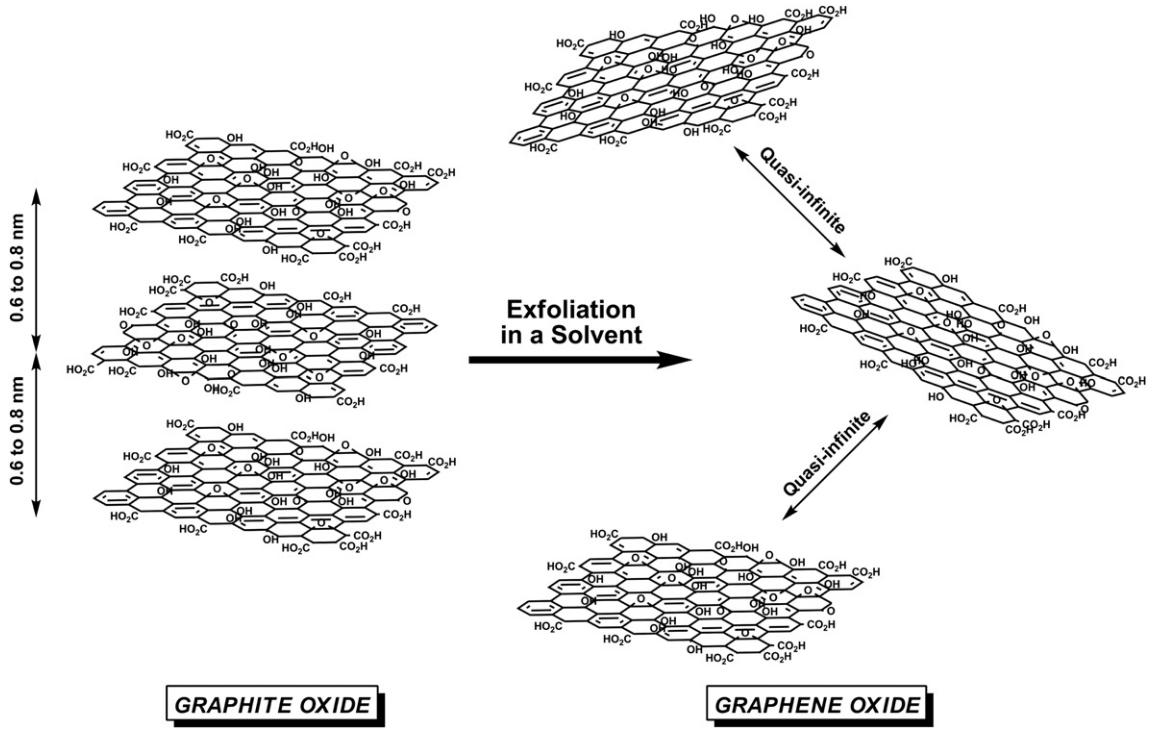

Fig. 1. Schematic illustrating the chemical structure of graphite oxide (GO) and the structural difference between layered GO and exfoliated graphene oxide (G–O) platelets.

exfoliation of GO prior to incorporation into a polymer matrix. Solvent-based exfoliation and thermal exfoliation techniques have emerged as two preferred routes for this step. In the former route, the hydrophilic nature and increased interlayer spacing of GO (relative to graphite) facilitates direct exfoliation into water assisted by mechanical exfoliation, such as ultrasonication and/or stirring, at concentrations up to 3 mg/ml, forming colloidal suspensions of 'graphene oxide' (that we define with the acronym 'G–O') [11]. Fig. 1 illustrates the structural difference between layered GO and exfoliated G–O platelets. Zeta potential measurements indicate that these suspensions are electrostatically stabilized by negative charges, possibly from the carboxylate groups that are believed to decorate the periphery of the lamellae [11]. Suspensions produced by sonication of GO are found, by atomic force microscopy (AFM) (when deposited onto various substrates), to consist primarily of single-layer G–O platelets [47,48] (Fig. 2); however, the sonication treatment fragments the platelets, reducing their lateral dimensions by over an order of magnitude down to a few hundred nanometers [8,49]. Mechanical stirring is an alternative route to produce single-layer G–O platelets of much larger lateral dimensions and aspect ratios when compared with G–O platelets produced by sonication. However, it has been reported that magnetic stirring exfoliates GO very slowly and in low yield [8]. GO can also be exfoliated to G–O platelets of similar aspect ratio to sonicated platelets (at lower concentrations below 0.5 mg/ml) via sonication in polar organic solvents such as DMF, PC, and NMP [50,51].

GO can also be exfoliated and reduced by rapid heating [45], yielding thermally expanded graphite oxide, or TEGO (also referred to commonly in the literature as functionalized graphene sheets, or FGS) [52,53]. In this exfoliation method, the dry powder is typically charged into a quartz tube (or other similar vessel) and subjected to thermal shock (i.e., exposure to a sudden jump in temperature), by heating to temperatures such as 400 °C [45] or higher [52] at high rates such as 2000 °C/min [52]. The rapid heating is believed to cause various small molecule species (e.g., CO, CO_2, water) to evolve and internal pressure to increase, forcing the sheets apart and yielding a dry, high-surface area material with a low bulk density (Fig. 2) [53]. Measurements of the surface area of TEGO by the Brunauer, Emmett, and Teller (BET) method [54] (which measures surface area based on isothermal gas adsorption/desorption) were found to range from 700 to 1500 m^2/g [52], compared with a theoretical limit of approximately 2600 m^2/g for graphene [55]. Also, GO can be exfoliated (and reduced) by microwave radiation, yielding a related material referred to as microwave-expanded graphite oxide, or MEGO [56]. Importantly, while G–O platelets are likely to maintain the chemical structure of GO, TEGO and MEGO are reduced (reported C:O ratios of 10:1 [52] and 3:1 [56], respectively), and are electrically conductive (reported values of roughly 2000 S/m [52] for TEGO [52] and 270 S/m for MEGO [56]). TEGO was reported to contain residual oxygen (in the form of carbonyl and ether groups) and adopted a crumpled accordion-like morphology, with lateral dimensions of a few hundred nanometers, similar to G–O platelets exfoliated by sonication [52,57].

2.5. Chemical reduction and functionalization of G–O platelets

The physical properties of G–O platelets are considerably different from that of graphene. G–O platelets can be chemically reduced to generate a material that resembles pristine graphene, using reducing agents such as hydrazine monohydrate or sodium borohydride [11]. Chemically reduced G–O platelets (henceforth, we will use the acronym RG–O) can exhibit C:O ratios of over 10:1 [8] and retain some of the functionality originally present on the G–O platelets [11,58]. Recently, it was reported that GO or G–O platelets may be used to catalyze the oxidation of a variety of benzylic and aliphatic alcohols [59], as well as various carbon–carbon bond forming reactions [60], while reducing GO as well as G–O platelets in the process. The products recovered after reduction by benzyl alcohol were reported to exhibit high C:O ratios (up to 29.9:1) and high electrical conductivities (up to 4600 S/m) [61]. Other reduction

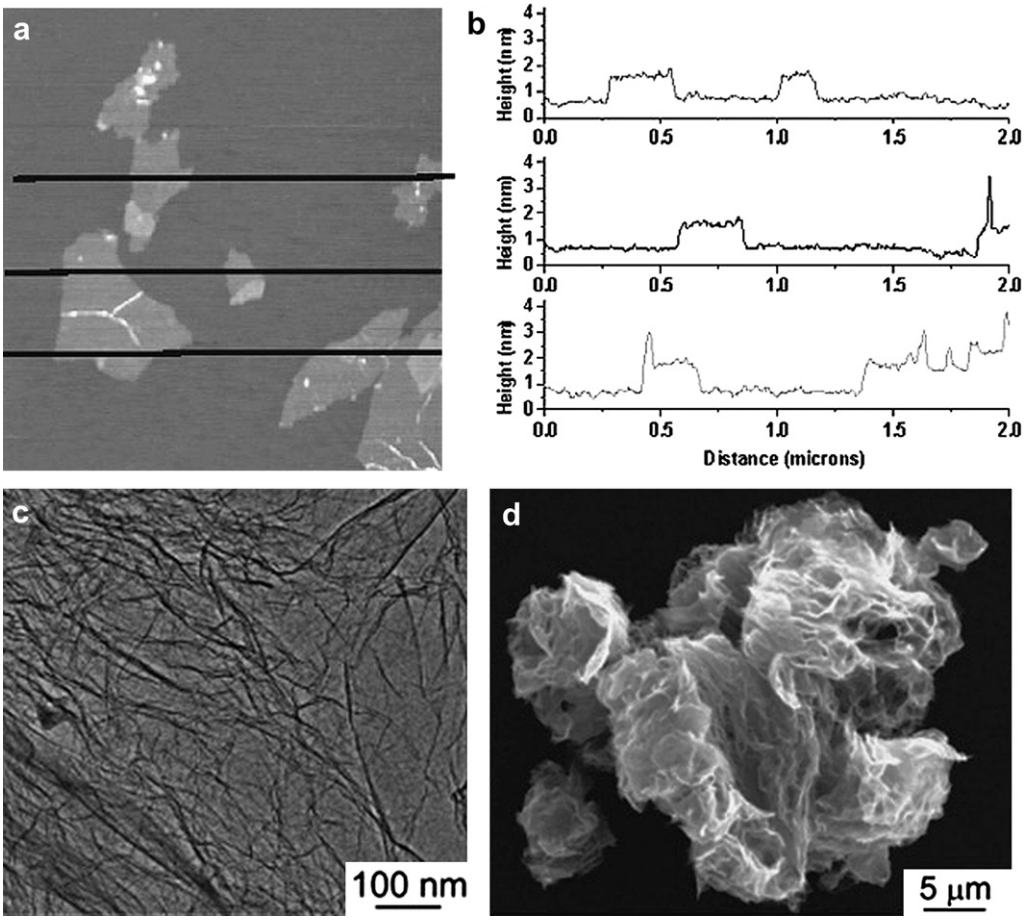

Fig. 2. (a, b) Non-contact AFM scans of graphene oxide (G–O) deposited on mica reveal the presence of single layers obtained from exfoliation in water via sonication. The wrinkled structure of thermally expanded GO (TEGO) is illustrated in this transmission electron micrograph (c) and scanning electron micrograph (d) ((a) and (b) were adapted from Ref. [64], (c) and (d) were adapted from Ref. [53]).

methods using environmentally friendly reductants, such as tryptophan and ascorbic acid, have been reported [62,63].

This reduction process can cause agglomeration of the platelets [64] (reducing accessible surface area) unless prior steps are taken to stabilize the suspension. Adjusting the pH of the suspension to increase the (negative) zeta potential of the sheets or the adsorption of polymers on the platelet surface are both effective routes to stabilizing aqueous suspensions of RG–O platelets [65,66]. Stable suspensions of RG–O platelets in organic solvents have also been achieved. One approach to these suspensions is progressive dilution of an aqueous suspension of G–O platelets with an organic solvent—with one possible route involving hydrazine in DMF:water (9:1 v/v) and further dilution in DMF to yield a stable suspension of RG–O platelets in 99% DMF [46]. Two-phase extraction of RG–O platelets from water into various organic solvents may be facilitated by end-functional polymers dissolved in the organic phase, which adsorb onto the platelets and help disperse the platelets in the solvent [67]. Freeze drying of aqueous RG–O dispersions has been reported to facilitate the re-dispersion of the RG–O platelets into organic solvents such as DMF [68]. Alternatively, one may avoid the use of water altogether, as stable dispersions of RG–O platelets in DMF and NMP have also been reported using dimethylhydrazine as the reductant [69]. For composites processed in solution, chemical reduction of G–O platelets in the polymer solution (provided the polymer is stable to the reaction conditions) may prevent the precipitation of the RG–O platelets from the solvent, as the polymer can maintain the dispersion of RG–O platelets [55].

While the most commonly employed reaction of G–O is its reduction to yield electrically conductive RG–O, a variety of other chemical transformations can be carried out at its oxygen-based functional groups, which are covered elsewhere [8]. Both covalent and non-covalent functionalization of G–O platelets has been reported to generate stable dispersions of chemically modified graphene (CMG) platelets in organic solvents and also to enhance their compatibility with various polymer matrices. Among others, reactions using amines [70–72] and isocyanates [73] have been reported for small molecule functionalization of G–O platelets because of the facility of the reactions, and the ability to react in multiple ways (e.g., amidations, nucleophilic epoxide ring-openings, carbamate formation, etc.) However, covalent functionalization of G–O platelets could adversely affect the electrical conductivity of the platelets as these functionalizations disrupt (or retain the disruption already present in) the sp^2-hybridized network required for good electron/hole conduction [74]. Non-covalent functionalization of RG–O platelets via, for example, π–π stacking could minimize disruption of the conductive, conjugated structure [75,76].

3. Preparation of graphene-based polymer nanocomposites

3.1. Overview and historical perspective

The earliest reports on polymer composites with exfoliated graphite fillers emerged from studies on the intercalation chemistry of GICs. In 1958, it was discovered that alkali metal-GICs could initiate the polymerization of ethylene [77], and subsequently, alkali

metal-GICs were found to initiate polymerization of other monomers such as styrene, methyl methacrylate, and isoprene [78,79]. Early reports focused on the characterization of the polymer produced from these reactions; it was decades later before the observation was reported that alkali metal-GIC-initiated polymerization could exfoliate the layers of the graphite host [37,80]. Building on his own work on the exfoliation of graphite, Bunnell proposed the production of polymer nanocomposites incorporating "as thin as possible" GNPs (derived from GICs exfoliated either by shear grinding or thermal treatment) as fillers in a 1991 patent [81], where he suggested that with "10 vol% inclusion of graphite flakes in…polyethylene or polypropylene, the stiffness of the finished product will approach that of aluminum." However, it was not until 2000 that a detailed study of the morphology and properties of an exfoliated graphite nanocomposite was published, which reported dispersed platelets of approximately 10 nm thickness, produced by exfoliation of EG due to the *in situ* polymerization of caprolactam [82]. This and subsequent studies have reported tremendous property improvements versus conventional polymer composites based on micron-scale fillers such as untreated flake graphite or carbon black (CB) [83–87]. For instance, much lower electrical percolation thresholds have been reported with GNP fillers versus CB: 8 wt% for CB/PMMA [88] and 9 wt% for CB/Nylon [89], compared with 1 wt% for GNP/PMMA [86] and 1.8 wt% for GNP/Nylon [82].

As with GICs, GO can be intercalated by various monomers, and subsequent polymerization has been reported to delaminate the layers [90]; however, it has also been reported that polymers can be directly intercalated into GO [91–93]. Hydrazine and electrochemical reduction of layered GO/polyelectrolyte films was used to generate electrically conductive polymer composites in 1996 [94], but it was nearly ten years later that an electrically conductive poly (styrene) composite was prepared by using well-dispersed, monolayer CMG fillers [55], stimulating an intense research effort on polymer composites with dispersed CMG platelets (and other GO-derived materials such as TEGO) as fillers.

In recent years, a variety of processing routes have been reported for dispersing both GNP and GO-derived fillers into polymer matrices. Many of these procedures are similar to those used for other nanocomposite systems [95], although some of these techniques have been applied uniquely to graphene-based composites. Among other factors, the nature of the bonding interaction at the interface between the filler and matrix has significant implications for the final composite properties, and most dispersion methods produce composites that are non-covalent assemblies where the polymer matrix and the filler interact through relatively weak dispersive forces. However, there is a growing research focus on introducing covalent linkages between graphene-based filler and the supporting polymer to promote stronger interfacial bonding, as will be illustrated in the following sections.

3.2. Non-covalent dispersion methods: solution and melt mixing

Solution-based methods generally involve the mixing of colloidal suspensions of G–O platelets or other graphene-based materials with the desired polymer, either itself already in solution or by dissolving in the polymer in the suspension of G–O platelets, by simple stirring or shear mixing. The resulting suspension can then be precipitated using a non-solvent for the polymer, causing the polymer chains to encapsulate the filler upon precipitation. The precipitated composite can then be extracted, dried, and further processed for testing and application. Alternatively, the suspension can be directly cast into a mold and the solvent removed. However, this latter technique can potentially lead to aggregation of the filler in the composite, which may be detrimental to composite properties [95].

Solution mixing has been widely reported in the literature, as CMG platelets can often be processed in either water or organic solvents. This approach has been used for incorporating GO-derived fillers into a variety of polymers, including: PS [55,96], polycarbonate [97], polyacrylamide [98], polyimides [99], and poly (methyl methacrylate) (PMMA) [7,100]. The facile production of aqueous G–O platelet suspensions via sonication makes this technique particularly appealing for water-soluble polymers such as poly(vinyl alcohol) (PVA) [100–105] and poly(allylamine), composites of which can be produced via simple filtration [104,106]. In addition, vacuum filtration of G–O/PVA and G–O/PMMA solutions has been used to make composite films across a broad range of loadings [107], which have a layered morphology similar to that of 'graphene oxide paper' [44].

While some restacking of the platelets may be possible, for solution mixing methods the dispersion of platelets in the composite is largely governed by the level of exfoliation of the platelets achieved prior to, or during, mixing. Thus, solution mixing offers a potentially simple route to dispersing single-layer CMG platelets into a polymer matrix. As previously mentioned, small molecule functionalization and grafting-to/from methods have been reported to achieve stable CMG platelet suspensions of highly exfoliated platelets prior to mixing with the polymer host. Lyophilization methods [68], phase transfer techniques [67,108], and surfactants [109] have all been employed to facilitate solution mixing of graphene-based composites. However, the use of surfactants may affect composite properties; for instance, surfactants have been reported to increase the matrix–filler interfacial thermal resistance in SWNT/polymer composites, attenuating the thermal conductivity enhancement relative to SWNTs that were processed without surfactants [110].

In melt mixing, a polymer melt and filler (in a dried powder form) are mixed under high shear conditions. Relative to solution mixing, melt mixing is often considered more economical (because no solvent is used) and is more compatible with many current industrial practices [111]; however, studies suggest that, to date, such methods do not provide the same level of dispersion of the filler as solvent mixing or *in situ* polymerization methods [26]. Notably, no means of dispersing single- or few-layer GO-derived fillers via melt mixing without prior exfoliation have been reported akin to layered silicate fillers (although, with a few exceptions, direct exfoliation of layered silicates in melt mixing requires prior treatment with a surfactant to increase miscibility with the polymer host [112]). Several studies report melt mixing using TEGO [113] and GNPs [114–117] as filler, where these materials could be fed directly into an extruder and dispersed into a polymer matrix without the use of any solvents or surfactants. Notably, the very low bulk density (approximately 0.004 g/cm^3 based on a volumetric expansion of 500 [52]) of TEGO makes handling of the dry powders difficult and poses a processing challenge (such as for feeding into processing equipment such as a melt extruder), and in one study a solution mixing process was used to disperse the TEGO in the polymer prior to compounding in order to circumvent this issue [118]. In a different approach to 'premix' the polymer and filler prior to mixing, GNPs were sonicated in a non-solvent, such that polymer particles were uniformly coated with GNPs prior to melt mixing, which was reported to lower the electrical percolation threshold of a GNP/polypropylene composite [119]. Notably, for composites incorporating G–O platelets as filler, melt processing and molding operations may cause substantial reduction of the platelets due to their thermal instability [120].

3.3. Non-covalent in situ polymerization

In situ polymerization methods for production of polymer composites generally involve mixing of filler in neat monomer

(or multiple monomers), or a solution of monomer, followed by polymerization in the presence of the dispersed filler. These efforts are often followed with precipitation/extraction or solution casting to generate samples for testing. Many reports using *in situ* polymerization methods have produced composites with covalent linkages between the matrix and filler, and many examples will be given in the following sections. However, *in situ* polymerization has also been used to produce non-covalent composites of a variety of polymers, such as poly(ethylene) [121], PMMA [122], and poly (pyrrole) [123,124].

Unlike what has been reported for solution mixing methods, a high level of dispersion of graphene-based filler has been achieved via *in situ* polymerization without a prior exfoliation step. In some reports, monomer is intercalated between the layers of graphite or GO, followed by polymerization to separate the layers. This technique, sometimes referred to as intercalation polymerization, has been widely investigated for nanoclay/polymer composites [112], and has been also applied to GNP and GO-derived polymer composites. For instance, *in situ* polymerization methods have been used to exfoliate GICs and EG to generate dispersions of GNPs in the matrix. Graphite can be intercalated by an alkali metal and a monomer (e.g., isoprene or styrene), followed by polymerization initiated by the negatively charged graphene sheets [37]. However, it is not known if the polymerization takes place on the surface of the GIC or between layers [37]. In any case, *in situ* polymerization in the presence of GICs has been reported to exfoliate the GIC into thin platelets [80], and this approach has also been reported to exfoliate EG [82,84,85], although exfoliation to afford isolated monolayers has yet to be achieved with this approach. In a recent study, metallocene-mediated polymerization of poly (ethylene) was conducted in the presence of dispersed GNPs, in an attempt to grow PE chains between the graphitic layers. Although the polymerization may have further exfoliated the GNPs, monolayer graphene platelets were not observed; TEM observations showed platelets down to 3.6 nm thickness (consistent with stacks of approximately 10 layers) with relatively low aspect ratios of about 30 dispersed in the PE matrix [121].

The larger interlayer spacing of GO (between about 0.6 and 0.8 nm depending on relative humidity) compared to graphite (0.34 nm) facilitates intercalation by both monomers and polymers [28]. Additionally, the polar functional groups of GO promote direct intercalation of hydrophilic molecules, with the interlayer spacing increasing with uptake of monomer or polymer (e.g., increasing up to 2.2 nm for the intercalation of PVA into GO) [93]. The interlayer spacing of vinyl acetate-intercalated GO was reported to decrease after polymerization [125], although the interlayer spacing still remains significantly higher than unmodified GO. *In situ* polymerization has been demonstrated for several GO composite systems, including poly(vinyl acetate) [125], and poly(aniline) (PANI) [90]. X-ray diffraction studies on these systems suggested an intercalated morphology where the individual graphene oxide sheets remain loosely stacked in the matrix with polymer intercalated between lamellae. However, the use of a macroinitiator to intercalate GO prior to *in situ* polymerization of methyl methacrylate was recently reported to improve the filler dispersion in a GO/PMMA composite. X-ray diffraction revealed an increased interlayer spacing of GO (from 0.64 nm to 0.8 nm) suggesting an intercalated morphology for GO/PMMA composites produced by conventional free radical polymerization. However, composites polymerized with the macroinitiator showed improved reinforcement and no diffraction peak from GO, suggesting a more exfoliated morphology [122].

3.4. Graphene-based composites with covalent bonds between matrix and filler

Given the relative sparseness of usable functionality on pure carbon materials, forming covalent linkages between the polymer matrix and such surfaces (when used as a composite filler) may be quite challenging. However, G–O platelets contain a surface rich in reactive functional groups, and a number of approaches for introducing covalent bonds between G–O platelets and polymers have been demonstrated. For instance, both grafting-from and grafting-to approaches have been used for the attachment of a broad range of polymers.

In one recent example of a grafting-from approach [126], atom transfer radical polymerization (ATRP) initiators were covalently attached via esterification with the alcohols present across the G–O platelet surface. Upon adding an ATRP-compatible monomer (e.g., styrene, butylacrylate, or methyl methacrylate) and a source of Cu^{I}, polymer brushes were grown in a controlled fashion from the surface (Fig. 3). The ester linkage between the polymer and the CMG platelet surface was then saponified using aqueous NaOH, allowing for characterization of the polymers independent of the carbon material. Similar studies using such ATRP-based methods have reported an increased scope of monomer reactivity [96,127], as well as the incorporation of these polymer-grafted CMG platelets

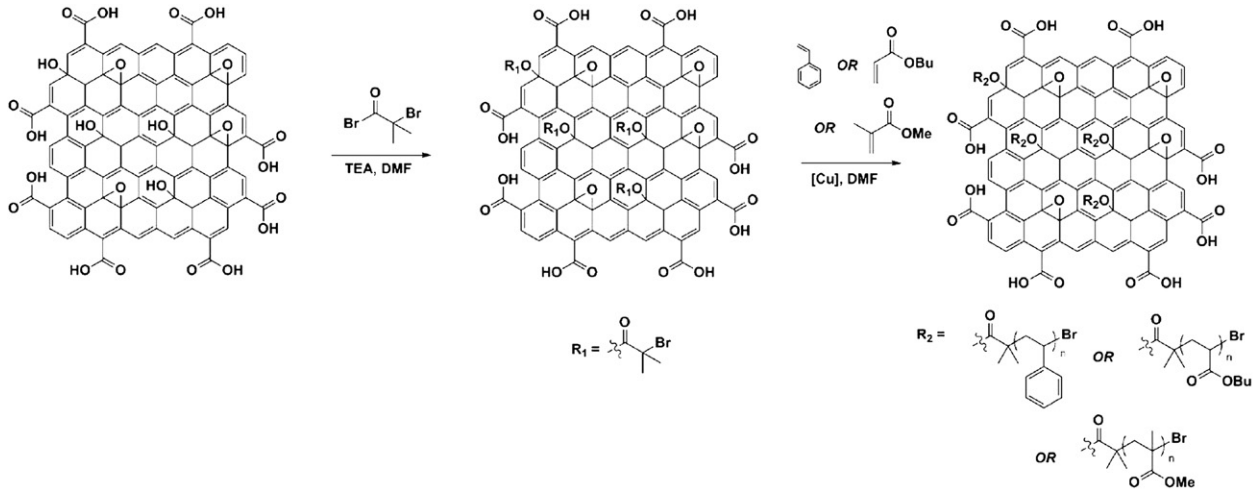

Fig. 3. Synthesis of surface-attached poly(styrene), poly(methyl methacrylate), or poly(butylacrylate) via ATRP following functionalization of G–O platelets with an ATRP initiator (α-bromoisobutyryl bromide) (adapted from Ref. [126]).

into a polymer matrix via solution mixing, reportedly leading to improvements in mechanical and thermal properties versus the neat matrix polymer [96,128,129]. Recent efforts have focused on correlation of thermal properties of these composites as a function of grafting density and polymer molecular weight [130].

These grafting-based approaches have also been used in conjunction with heterogeneous blending of polymer-functionalized G–O in matrices composed of conducting polymers [131], including poly(3-hexylthiophene) (P3HT) and a triphenylamine-based poly(azomethine) (see Fig. 4) [132,133]. Both polymers have been widely studied as conducting materials for use in photovoltaics and data storage devices, among other applications, and the incorporation of G–O platelets or other GO-derived materials into these devices may enhance the optoelectronic properties of the device, as well as enhance the device's mechanical and/or thermal properties. These two examples are good case studies for divergent pathways to polymer-functionalized G–O platelet composites: in the P3HT system, poly(*t*-butylacrylate) was grown via ATRP from the surface of G–O platelets (grafting-from, where a polymer is grown from a heterogeneous surface), and blended with pre-formed P3HT for the formation of organic electronic memory devices. Conversely, the poly(azomethine) was attached using the amino functional groups that were pendant to the end groups of the polymer (Fig. 4; grafting-to), possibly through amide formation with carboxylic acid groups present on the edges of G–O platelets. However, the presence of other reactive sites (e.g., epoxides) may make precise determination of the reactive site difficult [134]. Other reports of grafting-to approaches include reports of grafting of azide-terminated poly(styrene) (PS) chains to the surface of alkyne-functionalized G–O platelets via a Cu^{I}-catalyzed 1,3-dipolar cycloaddition in an example of click chemistry [135], and grafting of PVA to G–O platelets via carbodiimide-activated esterification [136]. The choice between using grafting-from or grafting-to methodologies will likely depend on the polymer being formed and which of the two approaches is more practical for the application under consideration. However, a grafting-to approach may lower the grafting density of chains to the platelet surface [137], which may in turn affect the dispersion of these polymer-grafted platelets if dispersed into a polymer matrix [138].

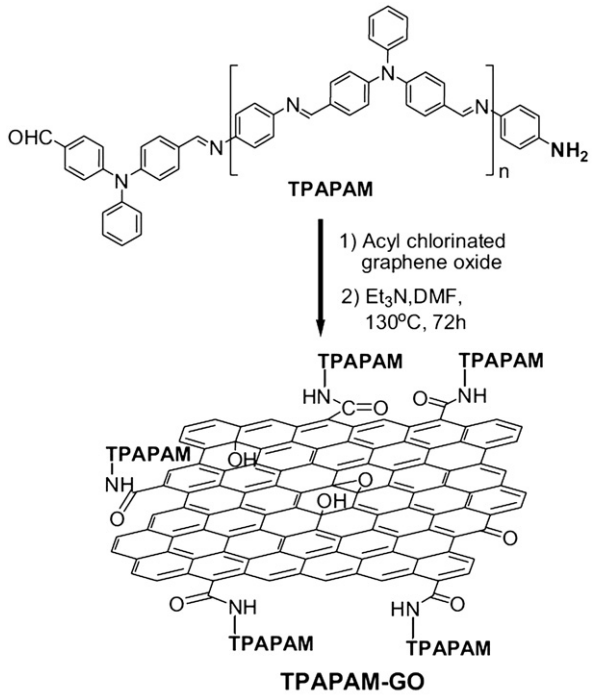

Fig. 4. Attachment of a triphenylamine-based poly(azomethine) (TPAPAM) to GO via amidation chemistry, embodying a grafting-to approach (adapted from Ref. [133]).

For certain polymers, covalent bonding between the matrix and G–O platelets may form during polymerization (on reaction with the functional groups of G–O) without the need for prior functionalization or controlled grafting methods. For an epoxy matrix composite, curing with an amine hardener may have resulted in the incorporation of G–O platelets directly into the crosslinked network [139], while for polyurethanes, TEGO was reported to function as a chain extender by reacting with the isocyanate groups of the monomer or prepolymer [26,140]. Ring-opening polymerization of caprolactam was reported to graft polyamide brushes to G–O platelets via condensation reactions between the amine-containing monomer and the carboxylic acid groups of the G–O platelets, though increased loadings of filler were found to lower the polymer molecular weight due to stoichiometric imbalance during polymerization [141].

G–O platelets have also been utilized as a Ziegler–Natta catalyst support for the heterogeneous *in situ* polymerization of propylene. Functionalization of G–O platelets with a Grignard reagent (BuMgCl) served to immobilize $TiCl_4$ on the G–O platelet surface (as evidenced by IR spectroscopy, X-ray photoelectron (XPS) spectroscopy, and energy-dispersive X-ray (EDX) spectroscopy). Subsequent initiation with $AlEt_3$ was reported to afford high molecular weight, isotactic poly(propylene) (Fig. 5). The resulting composites showed a homogeneous dispersion of few-layer CMG platelets, and exhibited moderate electrical conductivity (0.3 S/m at 4.9 wt%), with the authors noting that the G–O platelets were not intentionally reduced [142].

3.5. Other methods for composite preparation

In addition to those described above, several other methods have been reported for producing graphene-based composites. Although most of these procedures have been demonstrated on just one composite system, many could potentially find use as general approaches to composite fabrication. One such approach is the non-covalent grafting of well-defined polymers to RG–O platelets via π–π interactions. For instance, the attachment of pyrene-terminated poly(*N*-isopropylacrylamide) to RG–O was recently reported; the composite was stated to retain the thermoresponsive properties of the neat polymer [143]. This technique has since been extended to various other polymers [144], suggesting that non-covalent grafting of polymers to the surface of CMG platelets may provide a versatile approach to producing graphene-based composites. Moreover, such non-covalent composites may better preserve the conjugated structure of graphene-based materials as compared with covalent functionalization or grafting approaches, which may benefit composite properties such as electrical conductivity.

Variants of typical *in situ* polymerization and solution mixing methods may provide useful methods of dispersing graphene-based fillers in a polymer matrix. For instance, emulsion polymerizations can be carried out in aqueous suspensions of G–O platelets [145,146], suggesting a general approach for dispersion of CMG platelets with latex-based polymers [147]. As previously mentioned, lyophilization methods [68] or phase transfer techniques [67,108] may offer general approaches to dispersing RG–O platelets as filler in a polymer matrix. In one report, reduction of an aqueous suspension of G–O platelets with hydrazine resulted in the extraction of the hydrophobic RG–O platelets into an organic layer (containing the dissolved polymer) and formation of a homogeneously dispersed nanocomposite [108].

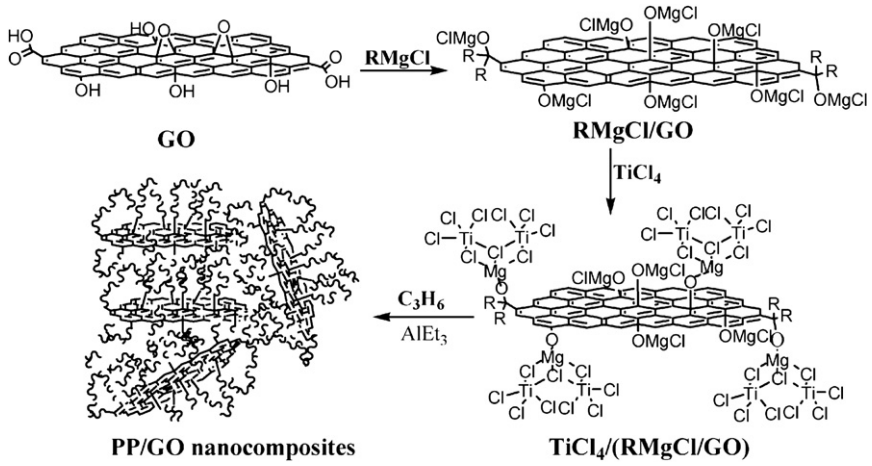

Fig. 5. Ziegler–Natta polymerization of propylene from the surface of G–O, which acts as a support for the growing polymer chains (adapted from Ref. [142]).

A variety of other methods for composite production have been reported. Attempts to exfoliate graphite directly via conventional melt mixing techniques have not been successful to date [148]. However, solid state shear pulverization, which uses a twin screw extruder to blend solid materials using shear, was reported to exfoliate and disperse unmodified graphite directly into polypropylene, yielding nanocomposites with platelets having thicknesses of approximately 10 nm or less [149]. Other production methods, such as layer-by-layer assembly of polymer composite films [150] and backfilling of G–O platelet aerogel structures (produced by freeze drying aqueous G–O suspensions) with polymer may provide means to produce nanocomposites with defined morphologies [151]. In one study, directional freeze drying of an aqueous G–O platelets/PVA platelets mixture was reported to yield nanocomposites with a three-dimensional macroporous structure and a surface area of approximately 37 m^2/g [152].

4. Morphology and crystallization behavior

As property enhancements correlate strongly with nanocomposite microstructure, effective characterization of morphology is important to establishing structure–property relationships for these materials. For instance, TEM of microtomed thin sections of the composite can provide direct observation of dispersed multilayer GNPs and graphene-based platelets; such thicker platelets typically show adequate contrast against the polymer matrix to be imaged without staining, whereas single-layer platelets may be difficult to directly observe by TEM [26]. Compared with TEM, wide-angle X-ray scattering (WAXS) can more rapidly provide insight into the state of dispersion over a larger volume of composite; however, since the scattering intensity varies with the concentration of the scattering feature, some morphological information may be missed [148].

Both graphite and GO, as the precursors to many graphene-based materials, have a layered structure as do certain silicates (e.g., montmorillonite) which have been widely investigated as composite fillers [111]. Indeed, when dispersed into a polymer matrix, both nanoclays and graphene-based platelets exhibit similar states of dispersion depending upon factors such as the processing technique and the affinity between the phases. Moreover, nanoclay fillers often exhibit comparable aspect ratios to graphene-based fillers (up to 1000) [112], although fillers such as TEGO often appear more crumpled on a local scale relative to nanoclays [7]. Earlier studies on nanoclay-based composites have suggested the existence of three general states of platelet dispersion on short length scales: stacked, intercalated, or exfoliated, as shown in Fig. 6. As similar morphologies have been observed in the literature on both GO-derived and GNP/polymer nanocomposites, we thus suggest extension of this terminology to these systems.

TEM and WAXS studies are perhaps the two most common means by which the state of dispersion can be assessed. Immiscibility of the phases and/or insufficient exfoliation of the graphite or GO-derived filler prior to mixing with polymer can result in large agglomerates consisting of stacked platelets when observed by TEM, which may also be suggested by the presence of a diffraction peak corresponding to the interlayer spacing of GO or graphite

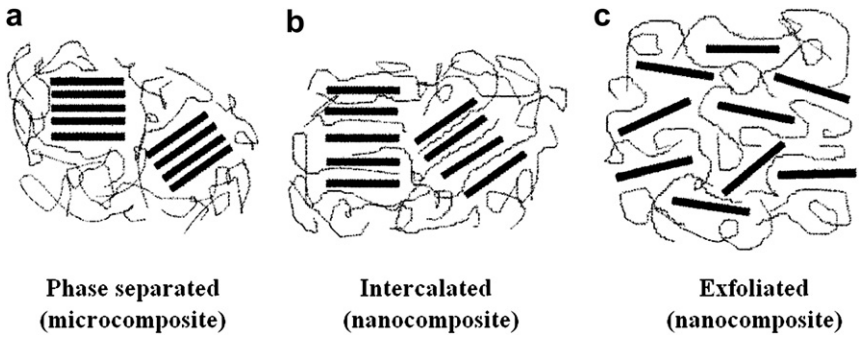

Fig. 6. Schematic showing three morphological states, as originally suggested for layered silicate fillers, that are also possible with graphene-based nanocomposites: (a) phase separated, (b) intercalated, (c) exfoliated (adapted from Ref. [23]).

[26,148,153]. Intercalated platelets retain a stacked structure but with increased interlayer spacing (on the order of a few nanometers), as evidenced by a shifted diffraction peak from that of unmodified graphite or GO [154]. As will be discussed in the following sections, high aspect ratio platelets are generally found to be beneficial to the mechanical, electrical, and thermal properties of a composite material. An exfoliated morphology of GO or GICs is thus usually desired as it provides higher aspect ratio platelets relative to stacked or intercalated platelets [155]. This state of dispersion may be suggested by a scattering profile corresponding to that of the neat matrix polymer; however, multi-layer intercalated platelets could actually be dispersed (as observed by TEM) despite the absence of a diffraction peak. Conversely, quantitative evaluation of platelet exfoliation and geometry via TEM poses its own set of challenges (such as sampling sufficient number of filler particles at such high magnification and the possible influence of TEM sample preparation on apparent level of dispersion).

While WAXS or TEM can be used to assess dispersion of individual platelets, neither can detect larger-scale morphological features [111,156]. Small-angle X-ray scattering (SAXS) and ultra-small-angle X-ray scattering (USAXS) measurements have been used on a variety of nanocomposite systems to detect the presence of fractal-like aggregates of filler at length scales beyond that of individual particles, although only limited information of this nature exists on GO-derived polymer composites [148], perhaps due in part to the limited accessibility of such techniques [111]. However, TEGO/polycarbonate nanocomposites were recently examined by small-angle neutron scattering. These measurements were used to quantify dispersion of the platelets (based on an idealized platelet model developed for montmorillonite), which suggested a decreasing effective aspect ratio with increased loading of TEGO and increased aggregation of filler at higher loadings [157]. Finally, cross-sectional analysis with scanning electron microscopy (SEM) has been used to evaluate dispersion of graphene-based filler [55] as well as to examine the surface for filler pull-out, possibly giving insight into the strength of interfacial adhesion [7,158]. However, care must be exercised when identifying the dispersed filler; moreover, SEM generally cannot resolve the degree of exfoliation of the platelets and is therefore best utilized as a complementary technique.

Exfoliated graphene-based materials are often compliant, and when dispersed in a polymer matrix are typically not observed as rigid disks, but rather as bent or crumpled platelets. Moreover, graphene has been shown to 'scroll up' irreversibly when its polymer host is heated above its glass transition temperature (T_g) [159]. Compatibility between the polymer matrix and the CMG platelets also can reportedly affect the platelets' conformation [160]. If the platelets' affinity for the matrix is high, then the particles may adopt a more extended conformation. However, the platelets may gradually adopt a more crumpled conformation as the affinity between the components decreases [160]. The technique used to process the composites can affect the microstructure, as shown in Fig. 7: randomly oriented, exfoliated platelets may be favored when composites are processed by solution mixing or *in situ* polymerization, compared with a more oriented and intercalated/stacked structure for composites produced by melt mixing, possibly due to restacking of the platelets [26]. The processing technique can also induce orientation of the dispersed platelets, which can be beneficial for reinforcement [161] but may raise the percolation threshold [153]. For composites processed by injection molding, platelets may be more randomly oriented near the interior of the specimen, with platelets aligned parallel to the surface [153]. By comparison, sufficiently thin, compression molded specimens [153] or solution-cast films [99] may have aligned platelets along the entire cross section. The filler type may also affect the orientation of the dispersed platelets. As shown in Fig. 8, solution-cast TEGO/Nafion composites exhibited a randomly oriented dispersion of TEGO platelets, whereas solution mixing of Nafion with G–O platelets, followed by hydrazine reduction, produced a highly oriented, uniform dispersion of RG–O platelets (it was stated that the reduction did not affect the orientation) [162]. The consequences of platelet conformations and orientations on composite properties will be discussed in more detail below.

For semicrystalline polymers, incorporation of a nanofiller can lead to an altered degree of crystallinity, crystallite size, spherulite structure, and may even induce crystallization of otherwise amorphous polymers [163,164]. Depending on the identity of the polymer, incorporation of graphene-based filler has been reported to cause increases [101,103,165,166], decreases [167], or no change [162] in the degree of crystallinity of a semicrystalline polymer matrix; changes in the polymer melting temperature have also been reported [168]. The presence of graphene-based nanofillers may also affect the rate of crystallization, by serving as a heterogeneous nucleation site for crystal growth [163]. Additionally, GNPs have been reported to accelerate the crystallite growth kinetics of poly (L-lactide), though the effect was found to be less pronounced than with carbon nanotubes (CNTs) [164].

Aside from crystallization, incorporation of graphene-based filler can impart other changes in the morphology of the polymer matrix or composite structure. The morphology of a self-assembling triblock copolymer, poly(styrene-*block*-isoprene-*block*-styrene), was stated to be affected by the presence of TEGO filler: AFM and electrostatic force microscopy (EFM) studies on approximately 300 nm-thick films prepared by spin coating revealed loss of long range order in the domains, with the TEGO preferentially dispersed in the PS blocks where they adopted a folded conformation [169]. Highly aligned G–O platelets dispersed in Nafion may have directed the orientation of the ionic domains of Nafion parallel to the surfaces of solution-cast films of the composites [162]. For electrospun graphene-based composites, a poor dispersion of CMG platelets has been reported to induce formation of bead-like structures in the fibers [170].

5. Rheological and viscoelastic properties

Study of nanocomposite rheology is important for the understanding of processing operations but it may also be used to examine nanocomposite microstructure [171–173]. In linear viscoelastic rheology measurements, the low-frequency moduli may provide information on the platelet dispersion; for instance, the presence of a low-frequency storage modulus (G') plateau is indicative of rheological percolation due to formation of a 'solid-like' elastic network of filler [174]; an example is illustrated in Fig. 9 for a TEGO/polycarbonate composite. The onset of a frequency-independent G' may also coincide with other phenomena, such as the loading at which a large decrease in the linear viscoelastic strain limit is observed [153]. The percolation threshold determined from such measurements can be used to roughly quantify dispersion in terms of an equivalent aspect ratio of idealized platelets [148,153]. Generally, G' has been found to increase across all frequencies with dispersion of rigid nanoplatelets, consistent with reinforcement. In addition to melt rheology, changes in the dynamic moduli have been studied in several composite systems with GNP and GO-derived fillers using dynamic mechanical analysis (DMA) temperature scans [175–178].

As previously mentioned, orientation of CMG platelets has been stated to affect the onset of rheological percolation, as randomly oriented, well-dispersed platelets would be expected to percolate at lower concentrations than aligned, well-dispersed platelets. One route to promoting the randomization of filler orientation is thermal annealing above the T_g of the polymer. As Fig. 9 shows, the

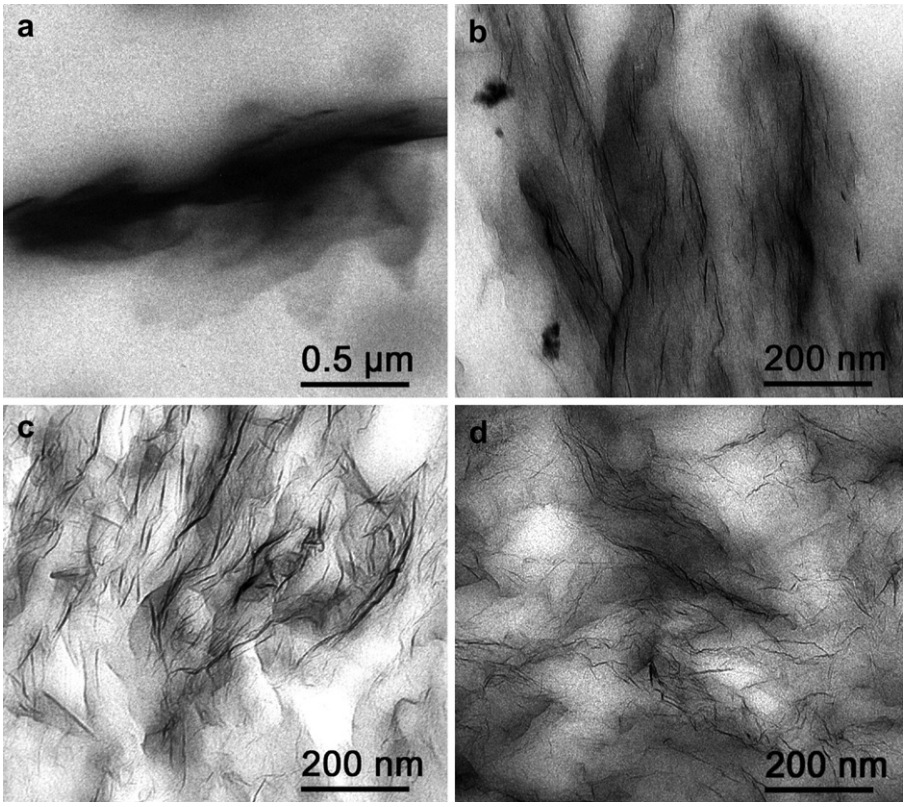

Fig. 7. TEM images illustrating the morphological differences in composites with a thermoplastic poly(urethane) matrix filled with (a) unexfoliated graphite in a stacked morphology, and (b) TEGO, processed by melt mixing. Images (c) and (d) show TEGO/polyurethane composites produced by solution blending and *in situ* polymerization, respectively, illustrating a more exfoliated state of dispersion (adapted from Ref. [26]).

rheological percolation threshold of a TEGO/polycarbonate composite was lowered from 1.5 vol% to 0.5 vol% by annealing for several hours [153]. Moreover, orientation of the platelets (induced by high strain) lowered the melt elasticity, while subsequent annealing steps were reported to restore the solid-like behavior of the composite melt. Hence, annealing of the composites following molding operations may provide a route to improve properties that benefit from randomly oriented (rather than aligned) platelets, such as the percolation threshold for electrical conductivity.

Lower composite solution viscosities have been reported with GNP fillers compared to CNTs [179], which may be advantageous for solution-based processing techniques, such as commercial molding processes for epoxy composite thermal interface materials. It has been suggested that at sufficiently high loadings, entanglement of CNTs in the matrix could result in undesirably large viscosity increases, whereas platelets can more easily slide past one another, thus moderating the viscosity increase [28]. Nonetheless, the solution viscosities of CMG/epoxy composites have been found to increase substantially with loading of filler, which could inhibit the formation of the crosslinked epoxy network [180]. It has been reported that functionalization to enhance compatibility of the filler with the polymer matrix may help to moderate the composite solution viscosity with increased loading [175]. Notably, GO composite solutions may exhibit electro-rheological properties, a characteristic of insulating colloidal particles in insulating media where increases in solution viscosity due to morphological changes can be observed upon application of an electric field [181].

6. Changes in the glass transition temperature

Low loadings of CMG fillers have been reported to cause large shifts in the T_g of the host polymer. This behavior has been explained,

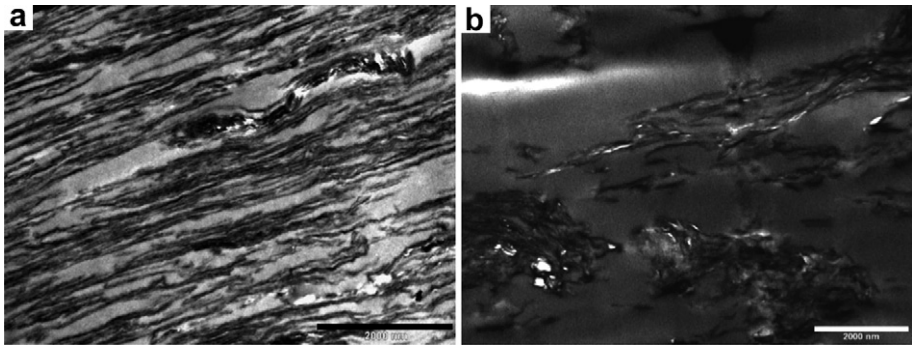

Fig. 8. TEM images contrasting (a) the preferential orientation of RG–O platelets parallel to the surface of a solution-cast RG–O/Nafion and (b) the randomly oriented dispersion of TEGO platelets in Nafion (scale bars = 2 μm; adapted from Ref. [162]).

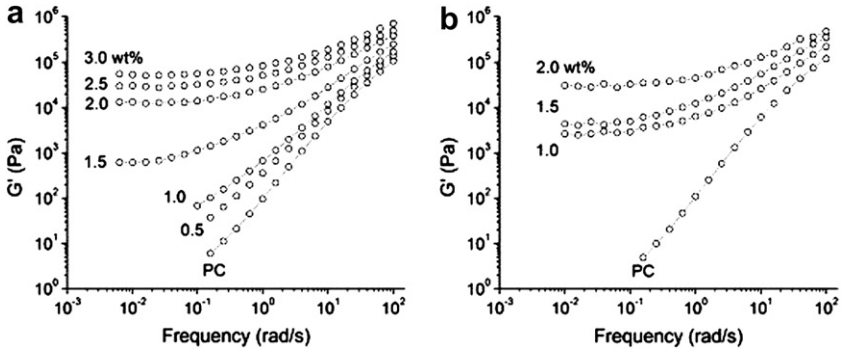

Fig. 9. Dynamic frequency sweeps of melt-blended TEGO/polycarbonate composite melts, illustrating the changes in low-frequency moduli of the composites after annealing times of (a) 10,000 s and (b) 20,000 s (adapted from Ref. [153]).

in general, by the altered mobility of polymer chains at an interface [163,182,183]. Fundamentally, an attractive polymer–matrix interface could restrict the chain mobility and thus tend to raise the T_g, whereas free surfaces and repulsive interfaces enhance chain mobility and lower the T_g; these mobility effects have been found to propagate away from the interface and gradually taper off with distance [184]. Depending on the strength of the interaction between the polymer and filler, this 'interphase' region of polymer chains with altered mobility may extend tens or even hundreds of nanometers away from the interface [185], potentially creating an enormous volume of polymer with significantly altered viscoelastic behavior. Formation of a network of interphase polymer may thus manifest large increases in the nanocomposite T_g at low loadings [186].

A striking example of this behavior was reported in nanocomposites of TEGO and poly(acrylonitrile) (PAN), where a shift in T_g of 40 °C at only 0.05 wt% loading of TEGO was observed [7]. In addition to the residual hydroxyl groups present on the TEGO surfaces promoting a positive T_g shift due to favorable non-covalent interactions with the polymer, the nanoscale roughness of the TEGO sheets was suggested to accentuate the effect [7]. T_g shifts have also been observed for CMG/polymer nanocomposites where the polymer is covalently bound to the platelet surface. In one report, G–O with PVA chains grafted to the surface via esterification was incorporated into a bulk PVA matrix, and the resulting composites showed a 35 °C shift in T_g [187]. Other reports on CMG composites with covalent matrix–filler interfaces have shown smaller but significant T_g shifts [96,188]; for such composites, it has been reported that higher grafting densities and lower molecular weight of grafted chains correlated with higher T_g values [130]. In general, T_g shifts over 20 °C are unusual—some studies have reported maximum T_g shifts between 10 and 20 °C [165,175,189], but many are lower still. Decreases in T_g have also been noted in composites which otherwise showed improvements in stiffness and electrical conductivity [157].

7. Electrical percolation and conductivity

One of the most promising aspects of graphene-based materials is their potential for use in device and other electronics applications, owing to their high electrical conductivity. 'Paper' materials made of stacked RG–O platelets have been reported to exhibit conductivities as high as 35,100 S/m [190], and such highly conductive materials, when used as fillers, may increase the bulk conductivity of an otherwise insulating polymer (e.g., poly(styrene) [55], poly(ethylene terephthalate) [113], etc.) by several orders of magnitude. In order for a nanocomposite with an insulating matrix to be electrically conductive, the concentration of the conducting filler must be above the electrical percolation threshold, where a conductive network of filler particles is formed [191]. As shown in Fig. 10, once electrical percolation has been achieved, the increase in conductivity as a function of filler loading can be modeled by a simple power-law expression

$$\sigma_c = \sigma_f(\phi - \phi_c)^t$$

where ϕ is the filler volume fraction, ϕ_c is the percolation threshold, σ_f is the filler conductivity, σ is the composite conductivity, and t is a scaling exponent. The filler need not be in direct contact for current flow; rather, conduction can take place via tunneling between thin polymer layers surrounding the filler particles, and this tunneling resistance is said to be the limiting factor in the composite conductivity [192,193]. Interestingly, recent work on TEGO/poly(vinylidene fluoride) (PVDF) nanocomposites showed a decrease in composite resistivity with increasing temperature (a negative temperature coefficient, or NTC, effect), which may suggest that for this system that the interplatelet contact resistance dominates over the tunneling resistance [177].

The electrical percolation thresholds achieved with graphene-based nanocomposites are often compared with those reported for CNT/polymer composites. Comparison of the sampling of percolation thresholds shown in Table 1 (representing the lowest threshold values reported to date) with comprehensive data

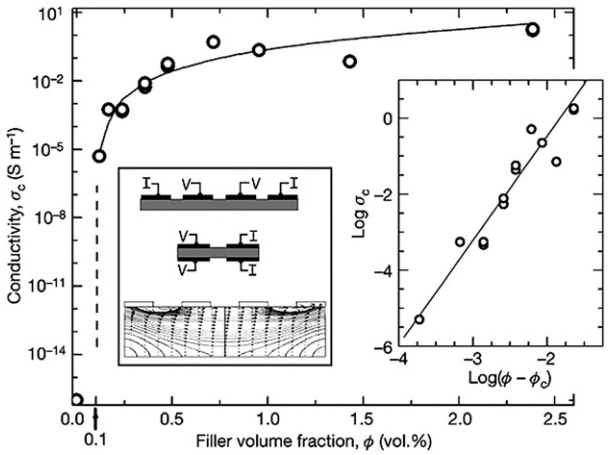

Fig. 10. Conductivity of composites of PS filled with phenyl isocyanate-functionalized RG-O versus filler volume fraction, illustrating the power-law dependence of conductivity above the percolation threshold ϕ_c (adapted from Ref. [55]).

Table 1
Values of the lowest electrical percolation thresholds and maximum electrical conductivities which have been reported in the literature for GNP and graphene-based nanocomposites for selected polymer matrices.

Matrix polymer	Filler type	Lowest percolation threshold reported (wt%)	Ref.	Filler type	Maximum conductivity (S/cm)[a]	Ref.
Epoxy	Funct. EG	1.0	[74]	RG–O	~0.05 (19 wt%)	[208]
Nylon-6	GO	0.5	[168]	GO	8.4×10^{-3} (1.8 wt%)	[168]
Poly(aniline) (doped)	GNP	0.7	[298]	GNP	522 (10 wt%)	[298]
Polycarbonate	TEGO	0.3	[157]	TEGO	0.5 (4.8 wt%)	[157]
Poly(ethylene)	RG–O	0.2	[198]	RG–O	0.1 (1.3 wt%)	[198]
Poly(ethylene terephthalate)	TEGO	1.0	[113]	TEGO	0.02 (6.5 wt%)	[113]
Poly(methyl methacrylate)	GNP	0.7	[84]	GNP	~1 (10 wt%)	[84]
Poly(propylene)	GNP	0.7	[119]	GNP	5×10^{-3} (10 wt%)	[119]
Poly(styrene)	Funct. G–O	0.2	[55]	RG–O	0.15 (2 wt%)	[147]
Poly(vinyl alcohol)	RG–O	0.5	[165]	RG–O	0.1 (7.5 wt%)	[165]
Poly(vinyl chloride)	GNP	1.4	[299]	GNP	0.06 (14.8 wt%)	[299]
Poly(vinylidene fluoride)	TEGO	2.0	[177]	TEGO	3×10^{-4} (4 wt%)	[177]
Polyurethane[b]	TEGO	0.6	[26]	TEGO	N/A (3.6 wt%)	[26]

[a] When loading was reported in volume percent, the density of bulk graphite (2.2 g/cm^3) was used to convert to a weight percent loading.
[b] Minimum resistance reported: ~200 Ω.

compiled on CNT-based nanocomposites [194] reveals that the lowest values reported for GNP- and graphene-based nanocomposites are, in general, somewhat higher than those reported for CNT-based composites. In particular, CNT/epoxy nanocomposites have been reported with electrical percolation thresholds as low as approximately 0.0025 wt% [195,196], far lower than has been reported for any graphene-based nanocomposite. These exceptional results have been ascribed to 'kinetic percolation' that most notably arises in composites with a low viscosity during processing (e.g., pre-cured epoxy), which can induce formation of a flocculated network of CNTs that electrically percolates at a much lower loading than possible with well-dispersed, randomly oriented fillers [156,197]. While comparison of the electrical percolation thresholds of composites is often valid, one must consider the influence of the sample geometry used for the conductivity measurements. For instance, a sufficiently long nanotube may be able to bridge between the electrodes for a sufficiently small test specimen, potentially suggesting a low percolation threshold which would otherwise not exist in a bulk composite specimen of much larger size.

It has been said that a high degree of dispersion may not necessarily yield the lowest onset of electrical percolation [156], as a sheath of polymer may coat the surfaces of well-dispersed filler and prevent direct interparticle contact. Indeed, the lowest percolation threshold achieved thus far for a graphene-based polymer nanocomposite (approximately 0.15 wt%; see Table 1) was observed when the filler was not homogeneously dispersed in the polymer matrix, but rather segregated from the matrix to form a conductive network [198]. In this study, poly(ethylene) particles were mixed with G–O in a water/ethanol mixture and were reduced using hydrazine, causing agglomeration of the RG–O and subsequent deposition onto the poly(ethylene) particles. This heterogeneous system was then hot pressed to generate a composite with a segregated, highly conducting network of RG–O filler [198]; however, such a morphology could compromise the composite's mechanical properties due to the agglomeration of filler [24]. In a related approach, an emulsion mixing method was used to coat polycarbonate microspheres with TEGO prior to compression molding which lowered the percolation threshold by over 50% versus a standard solution mixing method (to approximately 0.31 wt%, from 0.84 wt%) [157]. TEM observations showed a uniform dispersion of TEGO in the solution-mixed composites, compared with a segregated conductive network of TEGO in the emulsion-mixed composites, perhaps due to the exclusion of TEGO from the microspheres. Moreover, these composites (made by both dispersion methods) showed improved mechanical properties [157].

Alignment of the filler also plays a major role in the onset of electrical percolation: when the platelets are aligned in the matrix, there are, at least at relatively low concentrations, fewer contacts between them, and thus the percolation threshold would be expected to increase [199]. Compression molded polycarbonate and TEGO/polyester composites with aligned platelets were reported to show an electrical percolation threshold roughly twice that of annealed samples with randomly oriented platelets [148,153], while in another study, injection molding was reported to raise the percolation threshold over an order of magnitude versus compression molding for a GNP/poly(propylene) composite [119]. In general, the percolation threshold for electrical conductivity is often slightly higher than for rheological percolation, due to the requirement for closer proximity between platelets for particle tunneling (approximately 5 nm) for electrical percolation versus bridging by the interphase, which may extend over tens of nanometers [32,185,200]. In addition to lowering the percolation threshold, slight aggregation of the conductive filler may also improve the maximum electrical conductivities of these composites [194,201]. A combination of conductive carbon fillers may also be beneficial for lowering the electrical percolation threshold of graphene-based nanocomposites [202].

The electrical percolation threshold also depends on the intrinsic filler properties, and both theoretical models [203,204] and experiments [205] suggest that the electrical conductivity of a CMG/polymer nanocomposite depends strongly on the aspect ratio of the platelets, with a higher aspect ratio translating to a higher conductivity. Transistors produced using a phenyl isocyanate-functionalized RG–O/PS composite as the active layer reportedly exhibited an increased carrier mobility for composites containing larger-area platelets, suggesting that sheet–sheet junctions limit the composite conductivity [205] (Fig. 11). Wrinkled, folded, or otherwise non-ideal platelet conformations may also raise the electrical percolation threshold [206].

Aside from being used to impart electrical conductivity to an insulating polymer host, graphene-based fillers can also endow other unique electrical properties to composites. The positive temperature coefficient of resistivity of an RG–O/poly(ethylene) composite was stated to be tunable by varying the time of an isothermal heat treatment of the composite (at 180 °C), which was thought to randomize the RG–O network and raise the resistivity, thus raising the PTC [207]. Graphene-based composites are being explored for their dielectric properties [208], and in one study a large increase in the dielectric constant (up to 4.5×10^7 at 1000 Hz) was reported in a GNP/poly(vinylidene fluoride) composite near the percolation threshold of the composite [209].

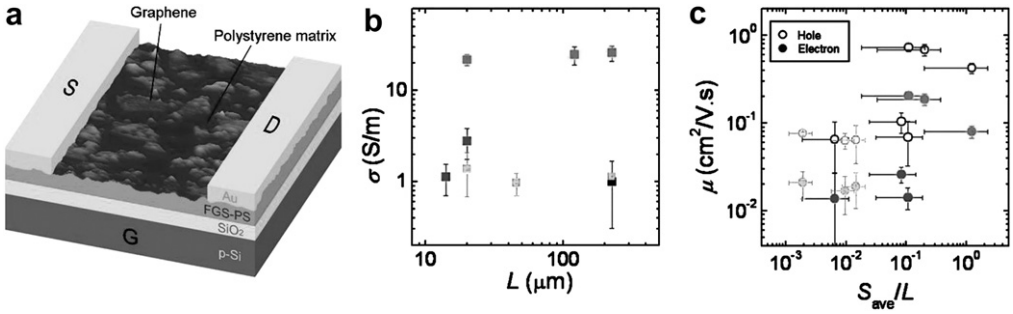

Fig. 11. (a) A transistor based off a phenyl isocyanate-functionalized RG–O/poly(styrene) composite shows different levels of (b) electrical conductivity and (c) carrier mobility depending on the aspect ratio of the platelets. The average lateral dimensions for the three platelet sizes studied were 0.44 μm, 1.5 μm, and 22.4 μm for the light grey, black, and medium grey points, respectively (adapted from Ref. [205]).

Notably, a variety of device applications have also been explored for graphene-based composites and these will be discussed in a following section.

8. Reinforcement and mechanical properties

The in-plane elastic modulus of pristine, defect-free graphene is approximately 1.1 TPa and is the strongest material that has ever been measured on a micron length scale [210]. CMG platelets exhibit an appreciably lower in-plane stiffness which calculations suggest may scale inversely with an increasing level of oxidation of the platelets [211]. A study using AFM nanoindentation on suspended CMG platelets reported the opposite, with the elastic modulus of the platelets evidently increasing with increasing oxidation level (decreasing conductivity), ranging from 250 GPa for RG–O platelets up to approximately 650 GPa for G–O platelets [22]. In another study, AFM tip-induced deformation on suspended platelets yielded an elastic modulus of monolayer G–O platelets of approximately 208 GPa. Moreover, the measurements revealed similar modulus values for two- and three-layer G–O platelets, at low strain [21]. These relatively large modulus values (compared to most polymeric materials), coupled with the large surface areas of the platelets, allow GO-derived fillers to be the primary load-bearing component of a polymer nanocomposite [161]. Fig. 12 provides an example of the reinforcing effect reported for RG–O/PVA composites.

Once dispersed in a polymer matrix, these compliant sheets or thin platelets commonly adopt wavy or wrinkled structures which may effectively reduce these modulus values [149], as crumpled platelets would tend to unfold rather than stretch in-plane under an applied tensile stress. Moreover, platelet restacking or incomplete exfoliation to single platelets could also lead to lower effective modulus values due to the decreased aspect ratios [161]. Highly crumpled conformations are often reported in composites using TEGO as filler, which along with structural defects generated during the high-temperature exfoliation processes [15], may significantly reduce the effective stiffness of the platelets and thus diminish their reinforcing capability. For instance, polycarbonate and poly (ethylene-2,6-naphthalate) (PEN) composites filled with TEGO showed only slightly larger modulus gains than composites reinforced with graphite at equivalent loadings, and calculations based on this experimental data suggested an effective modulus of around 70 GPa for TEGO—less than one-third of the measured value for single-layer RG–O [148,153]. Conversely, other studies have reported significant reinforcement from TEGO, attributed to strong interfacial bonding augmented by mechanical interlocking with the matrix due to the nanoscale roughness of the platelets [7,212]. Notably, the composites showing weaker reinforcement from TEGO were processed with melt mixing, which could possibly reduce the platelet aspect ratio (and thus reinforcement) due to particle attrition [32].

Aside from these issues with the intrinsic structure of GO-derived fillers, the reinforcing effectiveness observed from these materials thus far may be limited by problems with interfacial adhesion and spatial distribution of filler. Mechanical property enhancements have been found to correlate with improved nanofiller dispersion [23], and alignment of the filler in the matrix may increase reinforcement [161]. However, there is evidence that nanofillers (including CNTs and organoclays) which appear

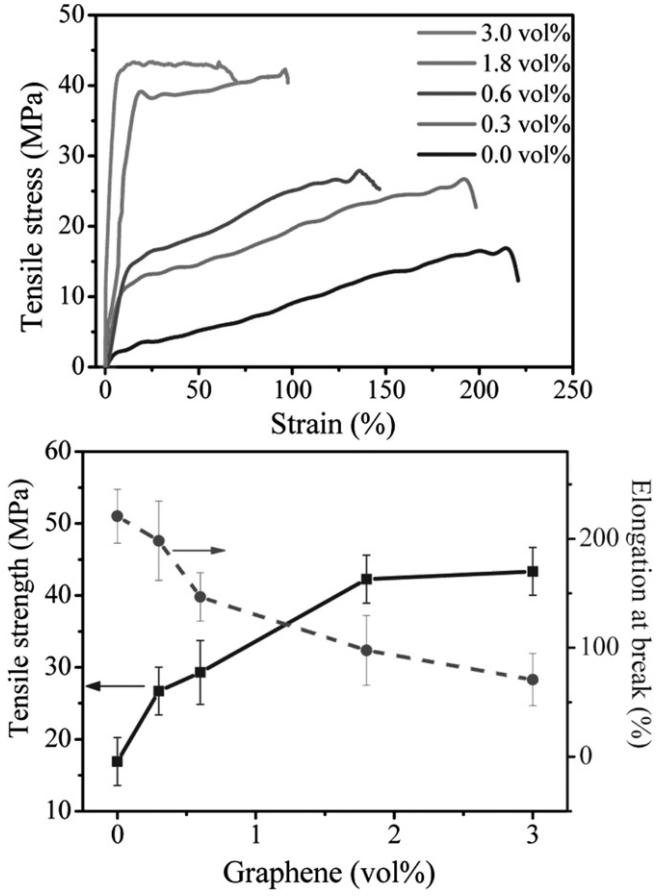

Fig. 12. Stress–strain plots of RG–O/poly(vinyl alcohol) composites as a function of filler loading, showing the pronounced reinforcing effect of RG–O. Tensile strength and elongation at break show opposing trends with increasing volume fraction of RG–O (adapted from Ref. [102]).

uniformly dispersed on short length scales may actually be aggregated into micron-scale fractal-like structures [156,213,214]. It has been suggested that such aggregates may be highly compliant and could reduce the effective aspect ratio of the filler, with both factors diminishing the reinforcing effect [156]. On the other hand, some have suggested that the presence of large-scale aggregates of filler is beneficial for reinforcement [138,215]. In any case, consideration of higher levels of nanocomposite structural hierarchy (as characterized by SAXS and USAXS, for example) may ultimately be necessary for extracting the full reinforcement potential of graphene-based fillers, and polymer-grafted platelets could potentially provide one route to tailoring the spatial distribution of filler [138,215].

Strong interfacial adhesion between the platelets and polymer matrix is also crucial for effective reinforcement [111,214,216–218]. Aside from making dispersion difficult, incompatibility between the phases may lower stress transfer due to low interfacial adhesion, resulting in a lower composite modulus [219]. Measurements of graphene-polymer interfacial adhesion have been carried out using AFM and Raman spectroscopy [220,221]. Evaluation of Raman spectra measured under strain revealed an interfacial shear stress of approximately 2.3 MPa in a graphene/PMMA composite (where the graphene was produced by micro-mechanical exfoliation) [220]. This value is similar to the value (2.7 MPa) of interfacial shear stress predicted by simulations of a poly(ethylene)/CNT nanocomposite with only van der Waals interactions between the matrix and filler [222], suggesting that the interaction between PMMA and the monolayer graphene platelets was also mediated by weak dispersive forces. By comparison, interfacial shear stresses up to 47 MPa have been measured for CNT/polymer composites [223] and values up to 500 MPa have been predicted for CNT-filled composites with covalent bonding at the matrix–filler interface [224]. These measurements thus suggest low levels of reinforcement for graphene-based polymer nanocomposites in the absence of covalent or stronger non-covalent bonding between the phases, emphasizing the importance of 'engineering' the filler–matrix interface in these systems.

Small molecule functionalization of graphene-based materials, either covalent or non-covalent, is a route to tailor the interface to promote stronger non-covalent interactions between the matrix and platelets [26]. Hydrogen bonding between GO-derived fillers and their polymer hosts has been cited as a major factor in large modulus and strength improvements observed in several polymers that can serve as hydrogen bond acceptors and/or donors [7,101,105,225]. Formation of a crystalline layer around the platelets by an isothermal treatment may also enhance stress transfer, as has been reported for a G–O/poly(caprolactone) composite [167]. Covalent bonding between the filler and matrix may provide the most effective means to increase the interfacial shear stress for improving stress transfer [218]. Monomers or chain extenders containing functional groups that can react directly with G–O in an *in situ* step-growth polymerization may thus covalently link G–O to the matrix; as recently reported for a G–O/Nylon-6 nanocomposite, this approach resulted in an unprecedented doubling of modulus and strength versus neat Nylon-6 at just 0.1 wt% loading [141]. The formation of covalent bonds between matrix and filler has also been reported to improve mechanical properties in epoxy and polyurethane composites with GNP and GO-derived fillers [26,74,140,226–228]. In addition, incorporation of polymer-grafted CMG fillers has been reported to greatly enhance the mechanical properties of PS [96], PMMA [129,188], and PVDF [128]. For such polymer-grafted fillers incorporated into a chemically identical polymer matrix, improvements in reinforcement may be strongly influenced by the relative molecular weights of the grafted polymer and matrix polymer [229].

Particularly large modulus gains have been reported in elastomeric matrices, most notably polyurethanes [26,140,226,227,230–232]. It has been pointed out that the pronounced modulus increases of elastomers may arise from the large difference in modulus between the filler and matrix—which also makes elastomers less sensitive to filler defects and non-ideal conformations than rigid thermoplastics—indeed, for graphene-based polyurethane composites the reinforcement effect was reported to be significantly attenuated above the soft segment T_g (approximately −30 °C) [26]. Increases in modulus of over two orders of magnitude (from approximately 10 MPa to 1.5 GPa at 55 wt% GNP [230]) have been reported in polyurethanes. In one study, moderate ductility was said to be retained despite the high loading, affording a composite with modulus and strength comparable to many rigid thermoplastics (e.g., polycarbonate) but with a much higher toughness and strain at break (15%) [230]. As shown in Fig. 13, TEGO/polyurethane composites made via *in situ* polymerization showed less improvement in modulus as compared with solution-mixed composites despite good dispersion, possibly due to chain extension by TEGO which may have inhibited formation of ordered, hydrogen-bonded hard segments [26]. In the case of a TEGO/silicone foam nanocomposite, densification of the composite relative to the neat foam may have complemented the effect of particle reinforcement, leading to the observed 200% increase in the normalized compressive modulus at just 0.25 wt% [233]. While the reported modulus increases are often significant, generally the remarkable ductility of elastomers is significantly compromised by incorporation of rigid filler; furthermore, graphene-filled elastomers often show a decline in tensile strength.

Beyond simple reinforcing effects, improvements in fracture toughness, fatigue strength, and buckling resistance have been noted in graphene-based composites [158,180,212,234–236]. At equivalent loadings, *in situ* polymerized TEGO/epoxy composites reportedly show a much higher buckling strength, fracture strength, and fracture energy than single- or multi-walled nanotubes-filled composites. In one study, a 94% increase in the fracture toughness of an CMG/epoxy composite versus neat epoxy was reported at 0.6 wt % loading. The toughness increase was attributed to the presence of pendant amine functionality on the CMG platelets potentially

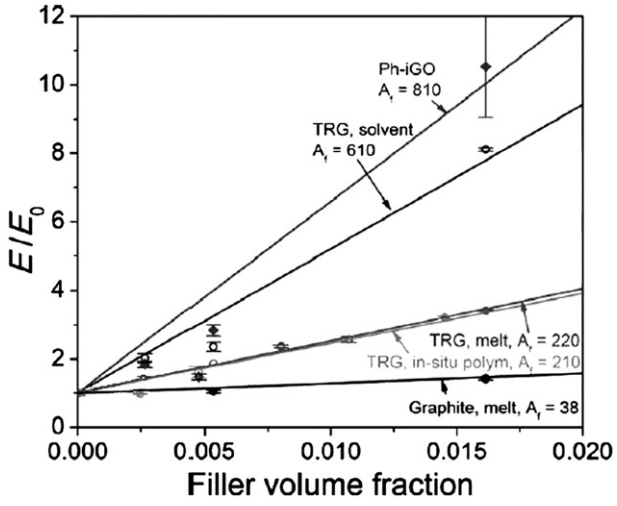

Fig. 13. Elastic moduli of polyurethane composites with flake graphite, TEGO ('TRG'), and phenyl isocyanate-functionalized G–O platelets (Ph–iGO) as filler, processed by either melt mixing, solvent mixing, or *in situ* polymerization (Ph–iGO composites were made by solution mixing). Fitting of the data to micro-mechanical models (solid lines) allows for calculations of effective aspect ratios (A_f) to quantify dispersion (adapted from Ref. [26]).

creating a "flexible interphase," although cross-linking between the CMG platelets may have also played a role [180]. Both increases [236] and decreases [237] in the impact strength of graphene-based composites have been reported.

As suggested above, GO-derived fillers could show superior reinforcement to layered clays due to their higher intrinsic stiffness. Calculations have suggested that randomly oriented graphene platelets may also produce nanocomposites with higher stiffness and strength than randomly oriented nanotubes, although calculations suggest that aligned CNTs may provide better reinforcement than aligned platelets at equivalent loading, aspect ratio, and dispersion [238]. Comparisons with GNP-filled composites [36,116,117,119,176,239] reveal that, generally, better mechanical properties are evidently achieved using well-exfoliated, GO-derived fillers at equivalent loadings. This may be primarily due to the relatively large platelet thicknesses (with a stacked structure) of GNP fillers, resulting in a lower aspect ratio and lower effective platelet modulus, thus decreasing their reinforcing effect. Notably, filler combinations such as SWNTs and TEGO [240] as well as TEGO and GO [241] may provide synergistic reinforcement, although the benefit (or lack of benefit) of these systems versus a single CMG filler at the same loading has not been fully established.

Comparisons of micro-mechanical predictions (e.g., Mori-Tanaka and Halpin-Tsai models) with experimental results on nanocomposites seem to indicate that reinforcement arises predominately from the native properties of the filler [111,161]. On the other hand, it has been suggested that the interphase concepts used to explain viscoelastic behavior may play a significant role in reinforcement owing to the modification of the properties of a large volume fraction of the matrix [163,216,242–244]. While these micro-mechanical models have been applied to some graphene-based composites in some reports [102,148,153], other results using GO-derived fillers have reportedly shown reinforcement at low loadings that exceed the upper-bound modulus predictions of these micro-mechanical models, perhaps suggesting a non-negligible contribution from the modified interphase matrix for such 'strongly bonded' systems [7,158]. Regardless, the apparent discrepancy between these results and theory highlights the need to develop further understanding of the relative contributions of native filler properties and changes in the polymer matrix in regards to the reinforcement of these systems.

9. Thermal conductivity, thermal stability, and dimensional stability

The exceptional thermal properties of GNPs and graphene-based materials have been harnessed as fillers to improve the thermal conductivity, thermal stability, and dimensional stability of polymers. Pristine graphene is highly thermally conductive; at room temperature, the thermal conductivity has been measured to be exceed 3000 W/m K when suspended [245,246] and approximately 600 W/m K when supported on a SiO_2 substrate [247]. CNTs show similar intrinsic thermal conductivities, but the sheet-like geometry of graphene-based materials may provide lower interfacial thermal resistance and thus produce larger conductivity improvements in polymer composites [248,249]. The geometry of graphite and graphene filler can also impart significant anisotropy to the thermal conductivity of the polymer composite [36], with the measured in-plane thermal conductivity as much as ten times higher than the cross-plane conductivity [250,251].

Many of the same considerations discussed for reinforcement and electrical conductivity apply for improving thermal conductivity. Close interparticle contact reduces thermal resistance and thermal conductivity in nanocomposites has been rationalized with percolation theory [252,253]. Since phonons are the primary mode of thermal conduction in polymers, covalent bonding between the matrix and filler can reduce phonon scattering at the matrix–filler interface, promoting higher composite thermal conductivity [175]. However, just as with electrical conduction, thermal conduction in nanocomposites can be compromised to some degree by platelet functionalization to enhance interfacial bonding [254].

Thermal conductivity studies of GNP and graphene-based composites have largely focused on epoxy matrix composites [175,179,248,250,255–257]. Significant improvements in thermal conductivity have been achieved in these systems (with composite conductivities ranging from 3 to 6 W/m K, up from approximately 0.2 W/m K for neat epoxy), but such large gains require relatively high carbon loadings (20 wt% and higher). Conductivities as high 80 W/m K at 64 wt% have been reported for GNP/epoxy composites, based on measurements of the thermal diffusivity [250]. The much smaller thermal conductivity contrast between polymer matrices and carbon nanofillers (as compared with electrical conductivity) may be the reason for the lower increases in thermal conductivity observed versus electrical conductivity at a given loading [95]. Different techniques have been utilized to lower the filler loading necessary to achieve large thermal conductivity gains. For instance, functionalization of EG with amine silyl groups improved the thermal conductivity by up to 20% over unmodified EG at the same loading [175]. A synergistic effect of combining SWNTs and GNPs (maximizing at a ratio of approximately 3:1 of GNPs:SWNTs) was reported, with TEM observations by the authors used to attribute the effect to the morphology of the filler blend in which the SWNTs bridged across adjacent GNP platelets, forming an extended network of filler in direct contact (Fig. 14) [248]. For G–O platelets with surface-initiated polymer brushes, higher composite thermal conductivities were reported to correlate with lower molecular weights of polymer and lower initiator grafting densities, perhaps illustrating the negative effect of excessive functionalization on thermal conduction [130].

A significant number of reports have reported increased thermal stability (as typically defined by the maximum mass loss rate measured by thermogravimetric methods) of polymers using GNPs and various CMGs as filler [114,116,170,177]; even GO can enhance the overall composite thermal stability versus the neat polymer [141,181], despite being thermally unstable itself. Studies on nanoclay-filled composites have suggested improved thermal stability trends with increased levels of exfoliation and interfacial

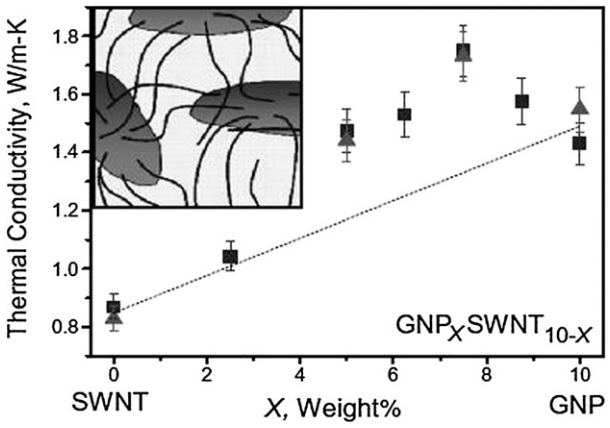

Fig. 14. Combination of graphite nanoplatelets (GNP) and single-walled carbon nanotubes (SWNTs) synergistically improve the thermal conductivity of epoxy. TEM studies established the presence of SWNTs bridging between dispersed GNPs (as shown in the schematic, inset) which may be responsible for the effect (adapted from Ref. [248]).

adhesion [258]. Most of these studies have focused on non-oxidative stability (heating under inert gas such as nitrogen or argon) and comparatively little data exists on the oxidative stability of GO composites. Increases in the onset of (non-oxidative) degradation of 20–30 °C and higher have been reported with GO-derived fillers [7,103,104,177]. However, GO is not always observed to confer thermal stability—in one case the presence of GO filler was found to accelerate the decomposition kinetics [259].

The negative coefficient of thermal expansion (CTE) of graphene [260,261], along with its high specific surface area and high stiffness, can significantly lower the coefficient of thermal expansion (CTE) of a polymer matrix [111]. In one study, the CTE of a G–O/epoxy composite was lowered by nearly 32% for temperatures below the T_g of the matrix at 5 wt% loading, although at 1 wt%, SWNTs produced a larger decrease in CTE than G–O platelets also loaded at 1 wt% (the two fillers were not compared at 5 wt%) [255]. Compared with CNTs, GNPs were reported to decrease the CTE of PP in two directions instead of one when aligned in the matrix [36].

10. Gas barrier properties

The incorporation of GNPs and GO-derived fillers can significantly reduce gas permeation through a polymer composite relative to the neat matrix polymer. A percolating network of platelets can provide a 'tortuous path' which inhibits molecular diffusion through the matrix, thus resulting in significantly reduced permeability (Fig. 15) [111]. Permeability studies on CMG/PS nanocomposites, however, suggest that at low loadings (e.g., below 0.05 vol%), the reduction in permeability of the composite is largely driven by a reduction in gas solubility in the composite, with diffusion effects becoming more important at higher loadings [262]. Orientation of the platelets may further enhance barrier properties perpendicular to their alignment, while higher platelet aspect ratios correlate with increased barrier resistance [111]. Notably, the one-dimensional geometry of CNTs may limit their effectiveness in improving the barrier properties of a composite relative to the neat polymer [26].

Both GNP and GO-derived fillers have been investigated in various permeation studies [26,36,114,115,153,262]; for thermoplastics, results include a 20% reduction in oxygen permeability for PP with 6.5 wt% GNP [36], and a 39% reduction in the nitrogen permeability of a polycarbonate/TEGO composite at approximately 3.5 wt% loading [153]. As shown in Fig. 15, CMG/PS composites were reported to show a lower oxygen permeability than exfoliated montmorillonite/PS composites at equivalent loadings [262]. In a comparative study of GO-derived fillers in thermoplastic polyurethanes, phenyl isocyanate-functionalized G–O platelets were reported to confer superior barrier properties relative to TEGO, with up to a 99% reduction in nitrogen permeability observed at approximately 3.7 wt% loading compared with an 81% reduction for TEGO at the same loading. Notably, the barrier properties in this study correlated with modulus improvements suggesting better filler alignment or higher aspect ratio for the functionalized G–O composites [26].

11. Applications of graphene-based polymer nanocomposites

Though numerous challenges remain in developing a fundamental understanding of GO-derived materials and their polymer composites, these materials have already been explored for a range of applications. Reflective of G–O's close relationship to graphene, many of the applications have focused on harnessing its electronic properties, particularly for devices. However, this is somewhat counterintuitive given that G–O is essentially an insulating material. For device applications, typically the G–O platelets and polymer are mixed and then the G–O platelets are reduced using hydrazine (or other strong chemical reductants) or thermal annealing, as discussed in the examples above.

One notable exception to this paradigm can be found in the development of an electronic memory device. Using the previously described surface-initiated polymerization methods, poly(*t*-butylacrylate) was reportedly grown from the surface of a thin film of G–O platelets [132]. The functionalized sheets were blended with P3HT and spun cast onto a surface of indium tin oxide (ITO), and then coated with a layer of aluminum. This device made use of the low conductivity of stacked and overlapped G–O platelets as a means of creating a barrier for inter-lamellar electron-hole recombination after excitons were formed. This created a clearly defined OFF state for the memory device. At the switching potential (found to be relatively high; −1.6 V), electrons were said to be excited from the HOMO of the P3HT portion of the mixture into the LUMO of the G–O platelet film/poly(*t*-butylacrylate) portion via intermolecular charge transfer. As the oxygen-containing functional groups of G–O platelets are believed to be inhomogeneously distributed across the lamellae [3], the excited electrons were able to travel relatively freely within the highly delocalized π-domains. Notably, the low bulk conductivity prevented recombination, resulting in a non-volatile memory storage system. This unique example took advantage of what is often perceived as a negative trait of G–O platelet material: its low conductivity. In contrast,

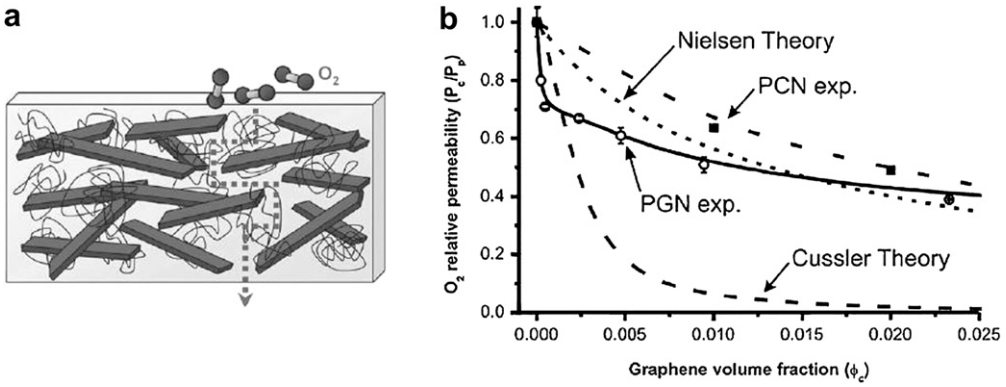

Fig. 15. (a) Illustration of formation of a 'tortuous path' of platelets inhibiting diffusion of gases through a polymer composite (Nielsen model). (b) Measurements of oxygen permeability of CMG/PS ('PGN') and montmorillonite/PS ('PCN') composites as a function of filler loading, compared with two theoretical models of composite permeability (adapted from Ref. [262]).

metal- and dopant-free conductive composites can be prepared from electrically conductive CMGs. These studies typically utilize the high degree of surface functionalization present on G–O platelets to attach polymers or polymerization initiators (grafting-to or grafting-from approaches, as previously discussed), followed by reduction of the oxidized surface to render the composite electrically conductive.

Field effect transistors (FETs) [205], solar cells (and other opto-electronic applications) [263], and energy storage devices [264] are three areas where such conductive composites may be particularly applicable. All of these applications capitalize upon the high conductivity inherent to many CMG composites. Photovoltaics and optoelectronics, in particular, rely on the fact that monolayers of graphene are about 98% transparent but still have high electrical conductivity. This feature makes graphene-based materials potentially well-suited to address issues related to photoexcitation and exciton mobility/diffusion as transparent conducting electrodes [265–268]. Overall efficiencies for these devices are still relatively low to date (typically less than 1% power conversion efficiency) when applied as organic photovoltaics, but this remains an area of interest particularly since the testing of these materials started so recently.

In addition to conductive polymers such as P3HT, graphene-based composites incorporating PANI have been studied as energy storage materials. Specific capacitances reported from 210 F/g to over 1000 F/g have been reported for these composites [269–274]. The precise reasons for this enhancement in energy storage capacity are still under investigation, but the authors state that this likely involves Faradaic transitions between the three different oxidation states of PANI (leucoemeraldine, emeraldine salt, and pernigraniline), in addition to the electrochemical double-layer capacitance (EDLC; general schematic shown in Fig. 16) provided by the carbon material [275]. It has been reported that PANI can intercalate into the layers of unexfoliated GO, increasing compatibility between the phases [181,276–278]. Even when GO was not reduced, the composite was rendered conductive by the PANI [276,277], though to a lesser extent than when RG–O platelets were incorporated [269].

Aside from devices, a host of diverse applications have been envisioned for graphene-based nanocomposites, all harnessing the property improvements discussed in the previous sections. For instance, the electrical conductivity of these composites may find use in electromagnetic wave interference shielding and anti-static coatings [208], while potentially maintaining properties of the host polymer such as transparency by virtue of the low percolation thresholds of these composite systems [55]. The combination of the improved barrier properties and increased light absorption of a CMG/PS composite versus neat PS suggests wider application as a packaging material [262]. The mechanical reinforcement achieved at low loadings of GO-derived filler offers potential uses in weight-sensitive aerospace and automotive applications such as tires, which could also benefit from the conductivity of RG–O platelets. Electrically conductive and robust GO-derived composite membranes could find use as capacitive pressure sensors in MEMS applications [279]. One less conventional application for these composites may be in self-healing materials [280,281]: very small loadings of multi-layer graphene in a shape memory epoxy matrix was reported to improve the composite's resistance to crack formation, thus enhancing scratch recovery upon heating above its T_g [282]. Interestingly, the filler used in this study was grown via microwave plasma-enhanced chemical vapor deposition, representing the first report of graphene composite filler generated from a 'bottom-up' synthesis route.

Nanofillers can also be used to reduce or overcome the intrinsic flammability of thermoplastics [111], and such applications have been explored for GO, despite the high flammability of GO when contaminated by synthetic byproducts such as potassium salts [283]. However, the thermal expansion of GO coupled with its evolution of gaseous byproducts (e.g., CO_2) at high temperatures may confer flame retardancy [284]. A recent study compared the fire retardancy of a GO/Nylon-6 composite to a nanoclay/Nylon-6 composite, and concluded that the volumetric expansion of GO particles conferred good short-term fire resistance, but the low structural integrity of the resulting material and release of oxidants on heating was a major disadvantage relative to nanoclays [285].

An emerging research direction for graphene-based composites is focused on biomedical applications. Graphene has been investigated for biosensor applications [286] and efforts have been directed at graphene-based composite biosensors as well [287–289]. Composite films of DNA and RG–O platelets have been prepared via solution mixing, and incorporation of other biological macromolecules along with DNA may provide a general approach to multifunctional, biocompatible composites [290]. A biocompatible hydrogel composite produced via physical cross-linking of PVA chains between G–O platelets showed a controlled release of Vitamin B12 depending on solution pH, and the authors stated this could find use in drug delivery [291]. Moreover, biocompatible free-standing composite films of poly(oxyethylene sorbitan laurate) (TWEEN) and RG–O could find use in transplant devices and implants [292]. Other biocompatible and biodegradable polymer composites have also been investigated, and incorporation of G–O

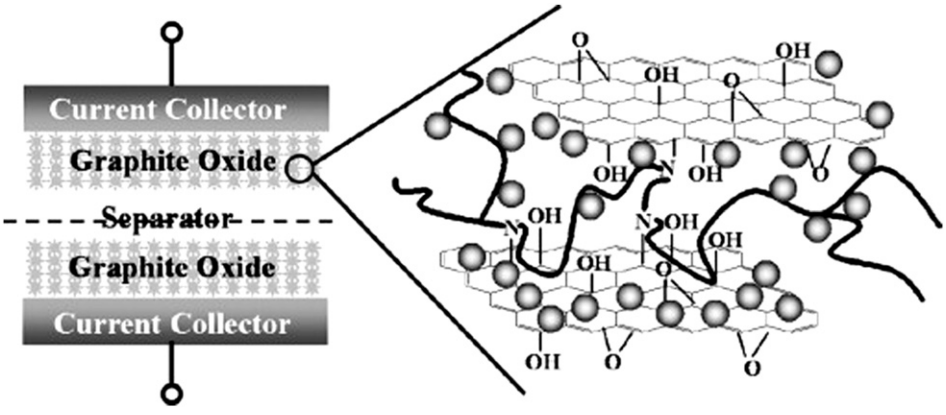

Fig. 16. Schematic of test electrochemical double-layer capacitor (EDLC) assembly and structural model of a GO/polymer composite assembled in the EDLC. The spheres in represent the electrolyte ions, which can be conveyed via diffusion and the segmental motion of the polymer chains (adapted from Ref. [264]).

platelets into chitosan [189,225] and poly(lactide) [114,164], in particular, may greatly expand the utility of these polymers that are otherwise limited by their mechanical properties.

12. Conclusions

Graphene-based polymer nanocomposites represent one of the most technologically promising developments to emerge from the interface of graphene-based materials and polymer materials. However, there are still many challenges that must be addressed for these nanocomposites to reach their full potential. For example, the sonication and thermal shock techniques commonly used to exfoliate GO also reduce the aspect ratio of the exfoliated platelets, which may negatively affect reinforcement as well as electrical and thermal properties [8,52]. Results suggesting poor interfacial adhesion in graphene/polymer composites in the absence of covalent bonding or additional non-covalent binding interactions such as $\pi-\pi$ interactions or hydrogen bonding underscore the importance of the platelet surface chemistry in reinforcement and the need for continued progress in this direction [220]. Moreover, the defects introduced into G–O platelets by either the oxidation to convert graphite to GO or the processing to generate G–O platelets, might ultimately limit the electrical conductivity and mechanical properties achievable with RG–O platelets relative to pristine and defect-free graphene platelets. Thus, methods of graphene platelet production which preserve its extended, conjugated structure may find favor for certain demanding applications of graphene-based composites [12].

Further property improvements in graphene-based composites will be influenced by improved morphological control. Defects and wrinkles in platelets are likely to influence their reinforcing capabilities, and so exfoliation and/or dispersion techniques that promote a more elongated morphology could conceivably further improve mechanical properties of these composites. Also, increased control over alignment and spatial organization of graphene-based fillers could be beneficial to nearly all types of composite properties. Thermal annealing of graphene-based composites to randomize GNP and graphene-based platelets may benefit the composite's electrical conductivity [153], whereas improved alignment of the platelets may improve reinforcement [161]. A variety of techniques for alignment of CNTs in polymer composites have been reported [293], and some of these techniques may find use for graphene-based composites. While the end application of graphene-based composites may dictate their specific morphological characteristics, the use of 'top-down' patterning or 'bottom-up' mesophase self-assembly approaches that have better morphological control could help to guide future studies of these systems, which may reveal new applications for these composites [213].

Despite these challenges, some of which are not unique to graphene-based nanocomposites, polymer nanocomposites have already found use in industry and their commercial impact is expected by many to rise significantly in the future [294]. As further improvements are made in the chemical production of graphene-based materials [295], composites using this class of filler could become a commercial reality. Notably, there is already significant effort and industrial interest in scaling up GO production [296]; GNP fillers have attracted similar attention [297]. Particularly relevant to large-scale production and transport of GO, flammability issues with this material have been identified and methods to alleviate these problems have been demonstrated [283]. Graphite, the precursor to GO and GO-derived fillers, is relatively cheap and abundant [296], and this cost factor will likely remain one of the primary advantages for using graphene-based fillers over CNTs in nanocomposites particularly as work on scale-up progresses. Furthermore, while CNTs and graphene reportedly offer comparable mechanical and electrical property enhancements, graphene-based materials appear to provide larger thermal conductivity enhancement as well as the advantage of improving barrier properties. The multifunctional property enhancements already demonstrated with graphene-based fillers, coupled with their potential for low cost and large-scale production, may expedite the applications of these nanocomposites as well as their transition to the marketplace.

Acknowledgements

This work was supported (in part) by the Laboratory Directed Research and Development (LDRD) program and the National Institute for Nano-Engineering at Sandia National Laboratories. Sandia is a multiprogram laboratory operated by Sandia Corporation, a Lockheed Martin Company, for the United States Department of Energy's National Nuclear Security Administration under Contract DE-AC04-94AL85000. CWB is grateful to the Robert A. Welch Foundation (F-1621) for support.

References

[1] Zhu Y, Murali S, Cai W, Li X, Suk JW, Potts JR, et al. Adv Mater 2010; 22:3906–24.
[2] Geim AK, Novoselov KS. Nat Mater 2007;6:183–91.
[3] Compton OC, Nguyen SBT. Small 2010;6:711–23.
[4] Carter LW, Hendricks JG, Bolley DS. 2531396, National Lead Company; 1950.
[5] Usuki A, Kojima Y, Kawasumi M, Okada A, Fukushima Y, Kurauchi T, et al. J Mater Res 1993;8:1179–84.
[6] Winey KI, Vaia RA. MRS Bull 2007;32:314–9.
[7] Ramanathan T, Abdala AA, Stankovich S, Dikin DA, Herrera-Alonso M, Piner RD, et al. Nat Nanotechnol 2008;3:327–31.
[8] Dreyer DR, Park S, Bielawski CW, Ruoff RS. Chem Soc Rev 2010;39:228–40.
[9] Kim H, Abdala AA, Macosko CW. Macromolecules 2010;43:6515–30.
[10] Dreyer DR, Ruoff RS, Bielawski CW. Angew Chem Int Ed 2010;49:9336–44.
[11] Park S, Ruoff RS. Nat Nanotechnol 2009;5:217–24.
[12] Dato A, Radmilovic V, Lee Z, Phillips J, Frenklach M. Nano Lett 2008;8:2012–6.
[13] Schafhaeutl C. J Prakt Chem 1840;21:129.
[14] Schafhaeutl C. Philos Mag 1840;16:570.
[15] Boehm HP, Clauss A, Fischer G, Hofmann U. Proceedings of the fifth conference on carbon; 1962.
[16] Boehm HP, Clauss A, Fischer GO, Hofmann U. Z Naturforsch 1962;17b:150–3.
[17] Boehm HP, Clauss A, Fischer GO, Hofmann U. Z Anorg Allg Chem 1962; 316:119–27.
[18] Allen MJ, Tung VC, Kaner RB. Chem Rev 2010;110:132–45.
[19] Loh KP, Bao Q, Ang PK, Yang J. J Mater Chem 2010;20:2277–89.
[20] Rafiee MA, Liu W, Thomas AV, Zandiatashbar A, Rafiee J, Tour JM, et al. ACS Nano; 2010. doi:10.1021/nn102529n.
[21] Suk JW, Piner RD, An J, Ruoff RS. ACS Nano; 2010. doi:10.1021/nl101902k.
[22] Gómez-Navarro C, Burghard M, Kern K. Nano Lett 2008;8:2045–9.
[23] Alexandre M, Dubois P. Mater Sci Eng R Rep 2000;28:1–63.
[24] Thostenson ET, Li CY, Chou TW. Compos Sci Technol 2005;65:491–516.
[25] Li D, Kaner RB. Science 2008;320:1170–1.
[26] Kim H, Miura Y, Macosko CW. Chem Mater 2010;22:3441–50.
[27] Dresselhaus MS, Dresselhaus G. Adv Phys 1981;30:139–326.
[28] Jang BZ, Zhamu A. J Mater Sci 2008;43:5092–101.
[29] Viculis LM, Mack JJ, Mayer OM, Hahn HT, Kaner RB. J Mater Chem 2005; 15:974–8.
[30] Chen G, Wu D, Weng W, Cuiling W. Carbon 2003;41:619–25.
[31] Li X, Zhang G, Bai X, Sun X, Wang X, Wang E, et al. Nat Nanotechnol 2008;3:538–42.
[32] Potschke P, Abdel-Goad M, Pegel S, Jehnichen D, Mark JE, Zhou DH, et al. J Macromol Sci Part A Pure Appl Chem 2010;47:12–9.
[33] Yasmin A, Luo J-J, Daniel IM. Compos Sci Technol 2006;66:1182–9.
[34] Zheng W, Lu X, Wong S-C. J Appl Polym Sci 2004;91:2781–8.
[35] Celzard A, Mareche JF, Furdin G, Puricelli S. J Phys D Appl Phys 2000; 33:3094–101.
[36] Kalaitzidou K, Fukushima H, Drzal LT. Carbon 2007;45:1446–52.
[37] Shioyama H. Synth Met 2000;114:1–15.
[38] Novoselov KS, Geim AK, Morozov SV, Jiang D, Zhang Y, Dubonos SV, et al. Science 2004;306:666–9.
[39] Zhang M, Parajuli RR, Mastrogiovanni D, Dai B, Lo P, Cheung W, et al. Small 2010;6:1100–7.
[40] Hernandez Y, Nicolosi V, Lotya M, Blighe FM, Sun Z, De S, et al. Nat Nanotechnol 2008;3:563–8.
[41] Lotya M, Hernandez Y, King PJ, Smith RJ, Nicolosi V, Karlsson LS, et al. J Am Chem Soc 2009;131:3611–20.
[42] Lu J, Yang J-X, Wang J, Lim A, Wang S, Loh KP. ACS Nano 2009;3:2367–75.

[43] Buchsteiner A, Lerf A, Pieper Jr A. J Phys Chem B 2006;110:22328–38.
[44] Dikin DA, Stankovich S, Zimney EJ, Piner RD, Dommett GHB, Evmenenko G, et al. Nature 2007;448:457–60.
[45] Ruess VG, Vogt F. Monatsh Chem 1948;78:222–42.
[46] Park S, An JH, Jung IW, Piner RD, An SJ, Li XS, et al. Nano Lett 2009;9:1593–7.
[47] Becerril HA, Mao J, Liu Z, Stoltenberg RM, Bao Z, Chen Y. ACS Nano 2008; 2:463–70.
[48] Gómez-Navarro C, Weitz RT, Bittner AM, Scolari M, Mews A, Burghard M, et al. Nano Lett 2007;7:3499–503.
[49] Li Z, Zhang W, Luo Y, Yang J, Hou JG. J Am Chem Soc 2009;131:6320–1.
[50] Paredes JI, Villar-Rodil S, Martinez-Alonso A, Tascon JMD. Langmuir 2008;24:10560–4.
[51] Zhu Y, Stoller MD, Cai W, Velamakanni A, Piner RD, Chen D, et al. ACS Nano 2010;4:1227–33.
[52] Schniepp HC, Li JL, McAllister MJ, Sai H, Herrera-Alonso M, Adamson DH, et al. J Phys Chem B 2006;110:8535–9.
[53] McAllister MJ, Li JL, Adamson DH, Schniepp HC, Abdala AA, Liu J, et al. Chem Mater 2007;19:4396–404.
[54] Brunauer S, Emmett PH, Teller E. J Am Chem Soc 1938;60:309–19.
[55] Stankovich S, Dikin DA, Dommett GHB, Kohlhaas KM, Zimney EJ, Stach EA, et al. Nature 2006;442:282–6.
[56] Zhu YW, Murali S, Stoller MD, Velamakanni A, Piner RD, Ruoff RS. Carbon 2010;48:2118–22.
[57] Bagri A, Mattevi C, Acik M, Chabal YJ, Chhowalla M, Shenoy VB. Nat Chem 2010;2:581–7.
[58] Boukhvalov DW, Katsnelson MI. J Am Chem Soc 2008;130:10697–701.
[59] Dreyer DR, Jia HP, Bielawski CW. Angew Chem Int Ed 2010;49:6813–6.
[60] Jia HP, Dreyer DR, Bielawski CW. Adv Synth Catal; 2011. doi:10.1039/adsc.201000748.
[61] Murali S, Dreyer DR, Zhu Y, Ruoff RS, Bielawski CW. J Mater Chem; 2011. doi:10.1039/C0JM02704A.
[62] Gao J, Liu F, Liu Y, Ma N, Wang Z, Zhang X. Chem Mater 2010;22:2213–8.
[63] Zhang J, Yang H, Shen G, Cheng P, Zhang J, Guo S. Chem Commun 2010; 46:1112–4.
[64] Stankovich S, Dikin DA, Piner RD, Kohlhaas KA, Kleinhammes A, Jia Y, et al. Carbon 2007;45:1558–65.
[65] Li D, Muller MB, Gilje S, Kaner RB, Wallace GG. Nat Nanotechnol 2008;3:101–5.
[66] Stankovich S, Piner RD, Chen X, Wu N, Nguyen SBT, Ruoff RS. J Mater Chem 2006;16:155–8.
[67] Choi EY, Han TH, Hong J, Kim JE, Lee SH, Kim HW, et al. J Mater Chem 2010; 20:1907–12.
[68] Cao Y, Feng J, Wu P. Carbon 2010;48:3834–9.
[69] Villar-Rodil S, Paredes JI, Martinez-Alonso A, Tascon JMD. J Mater Chem 2009;19:3591–3.
[70] Niyogi S, Bekyarova E, Itkis ME, McWilliams JL, Hamon MA, Haddon RC. J Am Chem Soc 2006;128:7720–1.
[71] Xu Y, Liu Z, Zhang X, Wang Y, Tian J, Huang Y, et al. Adv Mater 2009;21:1275–9.
[72] Liu Y, Zhou J, Zhang X, Liu Z, Wan X, Tian J, et al. Carbon 2009;47:3113–21.
[73] Stankovich S, Piner RD, Nguyen ST, Ruoff RS. Carbon 2006;44:3342–7.
[74] Miller SG, Bauer JL, Maryanski MJ, Heimann PJ, Barlow JP, Gosau JM, et al. Compos Sci Technol; 2010:1120–5.
[75] Su Q, Pang S, Alijani V, Li C, Feng X, Müllen K. Adv Mater 2009;21:3191–5.
[76] Xu Y, Bai H, Lu G, Li C, Shi G. J Am Chem Soc 2008;130:5856–7.
[77] Podall H, Foster WE, Giraitis AP. J Org Chem 1958;30:82–5.
[78] Panayotov IM, Rashkov IB. J Polym Sci Part A Polym Chem 1973;11:2615–22.
[79] Parrod J, Beinert G. J Polym Sci 1961;53:99.
[80] Shioyama H. Carbon 1997;35:1664–5.
[81] Bunnell LR. 5186919, Battelle Memorial Institute; 1993.
[82] Pan YX, Yu ZZ, Ou YC, Hu GH. J Polym Sci Part B Polym Phys 2000;38:1626–33.
[83] Chen G, Zhao W, editors. Nano- and biocomposites. CRC Press; 2009. p. 79–106.
[84] Chen G, Weng W, Wu D, Wu C. Eur Polym J 2003;39:2329–35.
[85] Chen G, Wu C, Weng W, Wu D, Yan W. Polymer 2003;44:1781–4.
[86] Zheng W, Wong S-C. Compos Sci Technol 2003;63:225–35.
[87] Zheng W, Wong S-C, Sue H-J. Polymer 2002;43:6767–73.
[88] Zois H, Apekis L, Omastova M. Proceedings – international symposium on electrets, 10th international symposium on electrets; 1999: pp. 529–532.
[89] Gabriel P, Cipriano LG, Ana JM. Polym Compos 1999;20:804–8.
[90] Liu P, Gong K. Carbon 1999;37:701–11.
[91] Kyotani T, Moriyama H, Tomita A. Carbon 1997;35:1185–7.
[92] Matsuo Y, Tahara K, Sugie Y. Carbon 1997;35:113–20.
[93] Matsuo Y, Hatase K, Sugie Y. Chem Mater 1998;10:2266–9.
[94] Kotov NA, Dékány I, Fendler JH. Adv Mater 1996;8:637–41.
[95] Moniruzzaman M, Winey KI. Macromolecules 2006;39:5194–205.
[96] Fang M, Wang KG, Lu HB, Yang YL, Nutt S. J Mater Chem 2009;19:7098–105.
[97] Higginbotham AL, Lomeda JR, Morgan AB, Tour JM. ACS Appl Mater Interfaces 2009;1:2256–61.
[98] Pandey R, Awasthi K, Tiwari RS, Srivastava ON. 2010; arXiv:1004.4281 [cond-mat.mes-hall].
[99] Chen D, Zhu H, Liu T. ACS Appl Mater Interfaces; 2010. doi:10.1021/am1008437.
[100] Das B, Prasad KE, Ramamurty U, Rao CNR. Nanotechnology 2009;20:125705.
[101] Liang JJ, Huang Y, Zhang L, Wang Y, Ma YF, Guo TY, et al. Adv Funct Mater 2009;19:2297–302.
[102] Zhao X, Zhang QH, Chen DJ, Lu P. Macromolecules 2010;43:2357–63.
[103] Yang X, Li L, Shang S, Tao X. Polymer 2010;51:3431–5.
[104] Xu YX, Hong WJ, Bai H, Li C, Shi GQ. Carbon 2009;47:3538–43.
[105] Jiang L, Shen XP, Wu JL, Shen KC. J Appl Polym Sci 2010;118:275–9.
[106] Satti A, Larpent P, Gun'ko Y. Carbon 2010;48:3376–81.
[107] Putz KW, Compton OC, Palmeri MJ, Nguyen SBT, Brinson LC. Adv Funct Mater 2010;20:3322–9.
[108] Wei T, Luo GL, Fan ZJ, Zheng C, Yan J, Yao CZ, et al. Carbon 2009;47:2296–9.
[109] Lee HB, Raghu AV, Yoon KS, Jeong HM. J Macromol Sci Part B Phys 2010;49:802–9.
[110] Bryning MB, Milkie DE, Islam MF, Kikkawa JM, Yodh AG. Appl Phys Lett 2005; 87:161909.
[111] Paul DR, Robeson LM. Polymer 2008;49:3187–204.
[112] Sinha Ray S, Okamoto M. Prog Polym Sci 2003;28:1539–641.
[113] Zhang HB, Zheng WG, Yan Q, Yang Y, Wang JW, Lu ZH, et al. Polymer 2010; 51:1191–6.
[114] Kim IH, Jeong YG. J Polym Sci Part B Polym Phys 2010;48:850–8.
[115] Jiang X, Drzal LT. Polym Compos; 2009:1091–8.
[116] Kim S, Do I, Drzal LT. Polym Compos 2010;31:755–61.
[117] Kalaitzidou K, Fukushima H, Drzal LT. Compos Part A Appl Sci Manuf 2007; 38:1675–82.
[118] Steurer P, Wissert R, Thomann R, Mulhaupt R. Macromol Rapid Commun 2009;30:316–27.
[119] Kalaitzidou K, Fukushima H, Drzal LT. Compos Sci Technol 2007; 67:2045–51.
[120] Jeong H-K, Lee YP, Jin MH, Kim ES, Bae JJ, Lee YH. Chem Phys Lett 2009;470:255–8.
[121] Fim FC, Guterres JM, Basso NRS, Galland GB. J Polym Sci Part A Polym Chem 2010;48:692–8.
[122] Jang JY, Kim MS, Jeong HM, Shin CM. Compos Sci Technol 2009;69:186–91.
[123] Gu Z, Zhang L, Li C. J Macromol Sci Part B Phys 2009;48:1093–102.
[124] Gu ZM, Li CZ, Wang GC, Zhang L, Li XH, Wang WD, et al. J Polym Sci Part B Polym Phys 2010;48:1329–35.
[125] Liu P, Gong K, Xiao P, Xiao M. J Mater Chem 2000;10:933–5.
[126] Lee SH, Dreyer DR, An JH, Velamakanni A, Piner RD, Park S, et al. Macromol Rapid Commun 2010;31:281–8.
[127] Yang YF, Wang J, Zhang J, Liu JC, Yang XL, Zhao HY. Langmuir 2009;25:11808–14.
[128] Layek RK, Samanta S, Chatterjee DP, Nandi AK. Polymer 2010;51:5846–56.
[129] Goncalves G, Marques PAAP, Barros-Timmons A, Bdkin I, Singh MK, Emami N, et al. J Mater Chem 2010;20:9927–34.
[130] Fang M, Wang KG, Lu HB, Yang YL, Nutt S. J Mater Chem 2010;20:1982–92.
[131] Zhang B, Chen Y, Zhuang XD, Liu G, Yu B, Kang ET, et al. J Polym Sci Part A Polym Chem 2010;48:2642–9.
[132] Li GL, Liu G, Li M, Wan D, Neoh KG, Kang ET. J Phys Chem C 2010;114:12742–8.
[133] Zhuang XD, Chen Y, Liu G, Li PP, Zhu CX, Kang ET, et al. Adv Mater 2010;22:1731–5.
[134] Park S, Dikin DA, Nguyen ST, Ruoff RS. J Phys Chem C 2009;113:15801–4.
[135] Sun ST, Cao YW, Feng JC, Wu PY. J Mater Chem 2010;20:5605–7.
[136] Veca LM, Lu FS, Meziani MJ, Cao L, Zhang PY, Qi G, et al. Chem Commun; 2009:2565–7.
[137] Coleman J, Khan U, Gun'ko Y. Adv Mater 2006;18:689–706.
[138] Akcora P, Kumar SK, Moll J, Lewis S, Schadler LS, Li Y, et al. Macromolecules 2010;43:1003–10.
[139] Yang H, Shan C, Li F, Zhang Q, Han D, Niu L. J Mater Chem 2009;19:8856–60.
[140] Lee YR, Raghu AV, Jeong HM, Kim BK. Macromol Chem Phys 2009; 210:1247–54.
[141] Xu Z, Gao C. Macromolecules 2010;43:6716–23.
[142] Huang YJ, Qin YW, Zhou Y, Niu H, Yu ZZ, Dong JY. Chem Mater 2010; 22:4096–102.
[143] Liu JQ, Yang WR, Tao L, Li D, Boyer C, Davis TP. J Polym Sci Part A Polym Chem 2010;48:425–33.
[144] Liu JQ, Tao L, Yang WR, Li D, Boyer C, Wuhrer R, et al. Langmuir 2010; 26:10068–75.
[145] Hu HT, Wang XB, Wang JC, Wan L, Liu FM, Zheng H, et al. Chem Phys Lett 2010;484:247–53.
[146] Zheming G, Ling Z, Chunzhong L. J Macromol Sci Part B Phys 2009; 48:226–37.
[147] Tkalya E, Ghislandi M, Alekseev A, Koning C, Loos J. J Mater Chem 2010; 20:3035–9.
[148] Kim H, Macosko CW. Macromolecules 2008;41:3317–27.
[149] Wakabayashi K, Pierre C, Dikin DA, Ruoff RS, Ramanathan T, Brinson LC, et al. Macromolecules 2008;41:1905–8.
[150] Wu JH, Tang QW, Sun H, Lin JM, Ao HY, Huang ML, et al. Langmuir 2008; 24:4800–5.
[151] Wang J, Ellsworth MW. ECS Trans 2009;19:241–7.
[152] Vickery JL, Patil AJ, Mann S. Adv Mater 2009;21:2180–4.
[153] Kim H, Macosko CW. Polymer 2009;50:3797–809.
[154] Kai W, Hirota Y, Hua L, Inoue Y. J Appl Polym Sci 2008;107:1395–400.
[155] Fu X, Qutubuddin S. Polymer 2001;42:807–13.
[156] Schaefer DW, Justice RS. Macromolecules 2007;40:8501–17.
[157] Yoonessi M, Gaier JR. ACS Nano; 2010. doi:10.1021/nn1019626.
[158] Rafiee MA, Rafiee J, Wang Z, Song HH, Yu ZZ, Koratkar N. ACS Nano 2009; 3:3884–90.
[159] Li Q, Li ZJ, Chen MR, Fang Y. Nano Lett 2009;9:2129–32.
[160] Hirata M, Gotou T, Horiuchi S, Fujiwara M, Ohba M. Carbon 2004;42:2929–37.
[161] Fornes TD, Paul DR. Polymer 2003;44:4993–5013.
[162] Ansari S, Kelarakis A, Estevez L, Giannelis EP. Small 2010;6:205–9.

[163] Schadler LS, Brinson LC, Sawyer WG. J Miner Met Mater Soc 2007;59:53–60.
[164] Xu JZ, Chen T, Yang CL, Li ZM, Mao YM, Zeng BQ, et al. Macromolecules 2010;43:5000–8.
[165] Salavagione HJ, Martinez G, Gomez MA. J Mater Chem 2009;19:5027–32.
[166] Cerezo FT, Preston CML, Shanks RA. Compos Sci Technol 2007;67:79–91.
[167] Cai DY, Song M. Nanotechnology 2009;20:315708.
[168] Du N, Zhao CY, Chen Q, Wu G, Lu R. Mater Chem Phys 2010;120:167–71.
[169] Peponi L, Tercjak A, Verdejo R, Lopez-Manchado MA, Mondragon I, Kenny JM. J Phys Chem C 2009;113:17973–8.
[170] Bao QL, Zhang H, Yang JX, Wang S, Tong DY, Jose R, et al. Adv Funct Mater 2010;20:782–91.
[171] Solomon MJ, Almusallam AS, Seefeldt KF, Somwangthanaroj A, Varadan P. Macromolecules 2001;34:1864–72.
[172] Wagener R, Reisinger TJG. Polymer 2003;44:7513–8.
[173] Zhang Q, Fang F, Zhao X, Li Y, Zhu M, Chen D. J Phys Chem B 2008; 112:12606–11.
[174] Vermant J, Ceccia S, Dolgovskij MK, Maffettone PL, Macosko CW. J Rheol 2007;51:429–50.
[175] Ganguli S, Roy AK, Anderson DP. Carbon 2008;46:806–17.
[176] Ramanathan T, Stankovich S, Dikin DA, Liu H, Shen H, Nguyen ST, et al. J Polym Sci Part B Polym Phys 2007;45:2097–112.
[177] Ansari S, Giannelis EP. J Polym Sci Part B Polym Phys 2009;47:888–97.
[178] Pramoda KP, Linh NTT, Tang PS, Tjiu WC, Goh SH, He CB. Compos Sci Technol; 2009:578–83.
[179] Yu A, Ramesh P, Itkis ME, Bekyarova E, Haddon RC. J Phys Chem C 2007; 111:7565–9.
[180] Fang M, Zhang Z, Li J, Zhang H, Lu H, Yang Y. J Mater Chem 2010;20:9635–43.
[181] Zhang WL, Park BJ, Choi HJ. Chem Commun 2010;46:5596–8.
[182] Bansal A, Yang H, Li C, Cho K, Benicewicz BC, Kumar SK, et al. Nat Mater 2005;4:693–8.
[183] Priestley RD, Ellison CJ, Broadbelt LJ, Torkelson JM. Science 2005;309:456.
[184] Ellison CJ, Torkelson JM. Nat Mater 2003;2:695–700.
[185] Rittigstein P, Priestley RD, Broadbelt LJ, Torkelson JM. Nat Mater 2007; 6:278–82.
[186] Qiao R, Catherine Brinson L. Compos Sci Technol 2009;69:491–9.
[187] Salavagione HJ, Gomez MA, Martinez G. Macromolecules 2009;42:6331–4.
[188] Pramoda KP, Hussain H, Koh HM, Tan HR, He CB. J Polym Sci Part A Polym Chem 2010;48:4262–7.
[189] Fan H, Wang L, Zhao K, Li N, Shi Z, Ge Z, et al. Biomacromolecules 2010; 11:2345–51.
[190] Chen H, Müller MB, Gilmore KJ, Wallace GG, Li D. Adv Mater 2008; 20:3557–61.
[191] Balogun YA, Buchanan RC. Compos Sci Technol; 2010:892–900.
[192] Roldughin VI, Vysotskii VV. Prog Org Coat 2000;39:81–100.
[193] Toker D, Azulay D, Shimoni N, Balberg I, Millo O. Phys Rev B Condens Matter Mater Phys 2003;68:41403.
[194] Bauhofer W, Kovacs JZ. Compos Sci Technol 2009;69:1486–98.
[195] Martin CA, Sandler JKW, Shaffer MSP, Schwarz MK, Bauhofer W, Schulte K, et al. Compos Sci Technol 2004;64:2309–16.
[196] Sandler JKW, Kirk JE, Kinloch IA, Shaffer MSP, Windle AH. Polymer 2003; 44:5893–9.
[197] Kovacs JZ, Velagala BS, Schulte K, Bauhofer W. Compos Sci Technol 2007; 67:922–8.
[198] Pang H, Chen T, Zhang G, Zeng B, Li ZM. Mater Lett 2010;64:2226–9.
[199] Haggenmueller R, Gommans HH, Rinzler AG, Fischer JE, Winey KI. Chem Phys Lett 2000;330:219–25.
[200] Du F, Scogna RC, Zhou W, Brand S, Fischer JE, Winey KI. Macromolecules 2004;37:9048–55.
[201] Hernández JJ, García-Gutiérrez MC, Nogales A, Rueda DR, Kwiatkowska M, Szymczyk A, et al. Compos Sci Technol 2009;69:1867–72.
[202] Wei T, Song L, Zheng C, Wang K, Yan J, Shao B, et al. Mater Lett 2010; 64:2376–9.
[203] Hicks J, Behnam A, Ural A. Appl Phys Lett 2009;95:213103.
[204] Li J, Kim JK. Compos Sci Technol 2007;67:2114–20.
[205] Eda G, Chhowalla M. Nano Lett 2009;9:814–8.
[206] Yi YB, Tawerghi E. Phys Rev E Stat Nonlin Soft Matter Phys 2009;79: 041134.
[207] Pang HA, Zhang YC, Chen T, Zeng BQ, Li ZM. Appl Phys Lett 2010;96:251907.
[208] Liang JJ, Wang Y, Huang Y, Ma YF, Liu ZF, Cai FM, et al. Carbon 2009; 47:922–5.
[209] He F, Lau S, Chan HL, Fan JT. Adv Mater 2009;21:710–5.
[210] Lee C, Wei X, Kysar JW, Hone J. Science 2008;321:385–8.
[211] Paci JT, Belytschko T, Schatz GC. J Phys Chem C 2007;111:18099–111.
[212] Rafiee MA, Rafiee J, Srivastava I, Wang Z, Song HH, Yu ZZ, et al. Small 2010;6:179–83.
[213] Vaia RA, Maguire JF. Chem Mater 2007;19:2736–51.
[214] Kluppel M, editor. The role of disorder in filler reinforcement of elastomers on various length scales, vol. 164. Springer; 2003. p. 86.
[215] Akcora P, Liu H, Kumar SK, Moll J, Li Y, Benicewicz BC, et al. Nat Mater 2009;8:354–9.
[216] Pukánszky B, Fekete E, editors. Adhesion and surface modification, vol. 139. Springer; 1999. p. 109–53.
[217] Lv C, Xue Q, Xia D, Ma M, Xie J, Chen H. J Phys Chem C 2010;114:6588–94.
[218] Wagner HD, Vaia RA. Mater Today 2004;7:38–42.
[219] Schadler LS, Giannaris SC, Ajayan PM. Appl Phys Lett 1998;73:3842–4.
[220] Gong L, Kinloch IA, Young RJ, Riaz I, Jalil R, Novoselov KS. Adv Mater 2010;22:2694–7.
[221] Cai M, Glover AJ, Wallin TJ, Kranbuehl DE, Schniepp HC. AIP Conf Proc 2010; 1255:95–7.
[222] Frankland SJV, Caglar A, Brenner DW, Griebel M. J Phys Chem B 2002; 106:3046–8.
[223] Barber AH, Cohen SR, Wagner HD. Appl Phys Lett 2003;82:4140–2.
[224] Wagner HD, Lourie O, Feldman Y, Tenne R. Appl Phys Lett 1998;72:188–90.
[225] Yang XM, Tu YF, Li LA, Shang SM, Tao XM. ACS Appl Mater Interfaces 2010;2:1707–13.
[226] Cai DY, Yusoh K, Song M. Nanotechnology 2009;20:085712.
[227] Nguyen DA, Lee YR, Raghu AV, Jeong HM, Shin CM, Kim BK. Polym Int 2009;58:412–7.
[228] Raghu AV, Lee YR, Jeong HM, Shin CM. Macromol Chem Phys 2008; 209:2487–93.
[229] Bansal A, Yang H, Li C, Benicewicz BC, Kumar SK, Schadler LS. J Polym Sci Part B Polym Phys 2006;44:2944–50.
[230] Khan U, May P, O'Neill A, Coleman JN. Carbon 2010;48:4035–41.
[231] Quan H, Zhang B-Q, Zhao Q, Yuen RKK, Li RKY. Compos Part A Appl Sci Manuf 2009;40:1506–13.
[232] Nguyen DA, Raghu AV, Choi JT, Jeong HM. Polym Polym Compos 2010;18:351–8.
[233] Verdejo R, Barroso-Bujans F, Rodriguez-Perez MA, de Saja JA, Lopez-Manchado MA. J Mater Chem 2008;18:2221–6.
[234] Rafiee MA, Rafiee J, Yu ZZ, Koratkar N. Appl Phys Lett 2009;95:223103.
[235] Yavari F, Rafiee MA, Rafiee J, Yu ZZ, Koratkar N. ACS Appl Mater Interfaces 2010;2:2738–43.
[236] Rafiq R, Cai D, Jin J, Song M. Carbon 2010;48:4309–14.
[237] Jiang X, Drzal LT. Polym Compos 2010;31:1091–8.
[238] Liu H, Brinson LC. Compos Sci Technol 2008;68:1502–12.
[239] Kim S, Drzal LT. J Adhes Sci Technol 2009;23:1623–38.
[240] Prasad KE, Das B, Maitra U, Ramamurty U, Rao CNR. Proc Natl Acad Sci USA 2009;106:13186–9.
[241] Jang JY, Jeong HM, Kim BK. Macromol Res 2009;17:626–8.
[242] Ciprari D, Jacob K, Tannenbaum R. Macromolecules 2006;39:6565–73.
[243] Putz KW, Palmeri MJ, Cohn RB, Andrews R, Brinson LC. Macromolecules 2008;41:6752–6.
[244] Jancar J, Douglas JF, Starr FW, Kumar S, Cassagnau P, Lesser AJ, et al. Polymer; 2010:3321–43.
[245] Balandin AA, Ghosh S, Bao W, Calizo I, Teweldebrhan D, Miao F, et al. Nano Lett 2008;8:902–7.
[246] Ghosh S, Calizo I, Teweldebrhan D, Pokatilov EP, Nika DL, Balandin AA, et al. Appl Phys Lett 2008;92:151911.
[247] Seol JH, Jo I, Moore AL, Lindsay L, Aitken ZH, Pettes MT, et al. Science 2010;328:213–6.
[248] Yu A, Ramesh P, Sun X, Bekyarova E, Itkis ME, Haddon RC. Adv Mater 2008;20:4740–4.
[249] Lin W, Zhang R, Wong CP. J Electron Mater 2010;39:268–72.
[250] Veca LM, Meziani MJ, Wang W, Wang X, Lu F, Zhang P, et al. Adv Mater 2009;21:2088–92.
[251] Ghose S, Watson KA, Working DC, Connell JW, Smith Jr JG, Sun YP. Compos Sci Technol 2008;68:1843–53.
[252] Zhong H, Lukes JR. Phys Rev B 2006;74:125403.
[253] Zhang G, Xia Y, Wang H, Tao Y, Tao G, Tu S, et al. J Compos Mater 2010; 44:963–70.
[254] Shenogin S, Bodapati A, Xue L, Ozisik R, Keblinski P. Appl Phys Lett 2004; 85:2229–31.
[255] Wang SR, Tambraparni M, Qiu JJ, Tipton J, Dean D. Macromolecules 2009; 42:5251–5.
[256] Debelak B, Lafdi K. Carbon 2007;45:1727–34.
[257] Hung MT, Choi O, Ju YS, Hahn HT. Appl Phys Lett 2006;89:023117.
[258] Leszczynska A, Njuguna J, Pielichowski K, Banerjee JR. Thermochim Acta 2007;453:75–96.
[259] Kaczmarek H, Podgórski A. Polym Degrad Stab 2007;92:939–46.
[260] Mounet N, Marzari N. Phys Rev B Condens Matter Mater Phys 2005;71:205214.
[261] Fasolino A, Los JH, Katsnelson MI. Nat Mater 2007;6:858–61.
[262] Compton OC, Kim S, Pierre C, Torkelson JM, Nguyen SBT. Adv Mater 2010;22:4759–63.
[263] Spitsina NG, Lobach AS, Kaplunov MG. High Energy Chem 2009;43:552–6.
[264] Tien CP, Teng HS. J Power Sources 2010;195:2414–8.
[265] Liu Z, He D, Wang Y, Wu H, Wang J. Sol Energy Mater Sol Cells; 2010:1196–200.
[266] Tung VC, Chen LM, Allen MJ, Wassei JK, Nelson K, Kaner RB, et al. Nano Lett 2009;9:1949–55.
[267] Valentini L, Cardinali M, Bon SB, Bagnis D, Verdejo R, Lopez-Manchado MA, et al. J Mater Chem 2010;20:995–1000.
[268] Geng X, Niu L, Xing Z, Song R, Liu G, Sun M, et al. Adv Mater 2010;22:638–42.
[269] Wu Q, Xu YX, Yao ZY, Liu AR, Shi GQ. ACS Nano 2010;4:1963–70.
[270] Wang D-W, Li F, Zhao J, Ren W, Chen Z-G, Tan J, et al. ACS Nano 2009; 3:1745–52.
[271] Wang H, Hao Q, Yang X, Lu L, Wang X. Electrochem Commun 2009; 11:1158–61.
[272] Yan J, Wei T, Shao B, Fan Z, Qian W, Zhang M, et al. Carbon 2010;48:487–93.
[273] Murugan AV, Muraliganth T, Manthiram A. Chem Mater 2009;21:5004–6.
[274] Bai H, Xu Y, Zhao L, Li C, Shi G. Chem Commun 2009;45:1667–9.
[275] Stejskal J, Gilbert J. Pure Appl Chem 2002;74:857–67.
[276] Higashkia S, Kimura K, Matsuo Y, Sugie Y. Carbon 1999;37:351–8.

[277] Wang H, Hao Q, Yang X, Lu L, Wang X. ACS Appl Mater Interfaces 2010; 2:821–8.
[278] Zhou X, Wu T, Hu B, Yang G, Han B. Chem Commun 2010;46:3663–5.
[279] Kulkarni DD, Choi I, Singamaneni SS, Tsukruk VV. ACS Nano 2010;4:4667–76.
[280] Williams KA, Boydston AJ, Bielawski CW. J R Soc Interface 2007;4:359–62.
[281] Williams KA, Dreyer DR, Bielawski CW. MRS Bull 2008;33:759–65.
[282] Xiao X, Xie T, Cheng YT. J Mater Chem 2010;20:3508–14.
[283] Kim F, Luo J, Cruz-Silva R, Cote LJ, Sohn K, Huang J. Adv Funct Mater; 2010. doi:10.1002/adfm.201000736.
[284] Rothon RN. In: Jancar J, editor. Mineral fillers in thermoplastics: filler manufacture and characterisation, vol. 139. Springer; 1999. p. 67–108.
[285] Dasari A, Yu ZZ, Mai YW, Cai GP, Song HH. Polymer 2009;50:1577–87.
[286] Wenrong Y, Kyle RR, Simon PR, Pall T, Gooding JJ, Filip B. Angew Chem Int Ed 2010;49:2114–38.
[287] Lu J, Do I, Drzal LT, Worden RM, Lee I. ACS Nano 2008;2:1825–32.
[288] Lu J, Drzal LT, Worden RM, Lee I. Chem Mater 2007;19:6240–6.
[289] Zhou KF, Zhu YH, Yang XL, Luo J, Li CZ, Luan SR. Electrochim Acta 2010; 55:3055–60.
[290] Patil AJ, Vickery JL, Scott TB, Mann S. Adv Mater 2009;21:3159–64.
[291] Bai H, Li C, Wang X, Shi G. Chem Commun 2010;46:2376–8.
[292] Park S, Mohanty N, Suk JW, Nagaraja A, An J, Piner RD, et al. Adv Mater 2010; 22:1736–40.
[293] Xie XL, Mai YW, Zhou XP. Mater Sci Eng R Rep 2005;49:89–112.
[294] Hussain F, Hojjati M, Okamoto M, Gorga RE. J Compos Mater 2006;40:1511–75.
[295] Marcano DC, Kosynkin DV, Berlin JM, Sinitskii A, Sun Z, Slesarev A, et al. ACS Nano 2010;4:4806–14.
[296] Segal M. Nat Nanotechnol 2009;4:611–3.
[297] University MS http://research.msu.edu/techtransfer/1-mil-support-msu-spinoff-xg-sciences. [accessed 30.07.10].
[298] Wu X, Qi S, He J, Duan G. J Mater Sci 2010;45:483–9.
[299] Vadukumpully S, Paul J, Mahanta N, Valiyaveettil S. Carbon 2011;49:198–205.

Jeffrey R. Potts is a Ph.D. student in materials science at the University of Texas at Austin working with Prof. Rodney S. Ruoff. He received his B.S. from Oklahoma State University in 2008 where he conducted research in Raman and photoluminescence spectroscopy with Prof. Don A. Lucca. He is a part of the National Institute for Nano-Engineering (NINE) program at Sandia National Laboratories (NM), where he works on chemically modified graphene materials for stimuli-responsive nanocomposites. His current research focus is on the synthesis and characterization of graphene-based materials and their incorporation into polymers to form nanocomposites.

Daniel R. Dreyer is a Ph.D. candidate in the chemistry program at the University of Texas at Austin studying under Prof. Christopher W. Bielawski. He received his B.S. in chemistry from Wheaton College (IL) in 2007 where he conducted research in confocal microscopy under Prof. Daniel L. Burden. During his undergraduate career he also studied X-ray reflectometry and plasma polymerization under Prof. Mark D. Foster at the University of Akron as part of an NSF-sponsored REU. His current research interests include applications of ionic liquids in synthetic polymer chemistry, structurally dynamic/self-healing materials, and carbon materials for use in catalysis and energy storage devices.

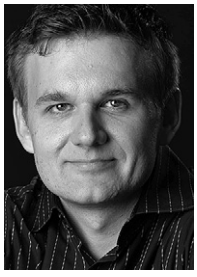

Christopher W. Bielawski received a B.S. degree in chemistry from the University of Illinois at Urbana-Champaign (1996) and a Ph.D. in chemistry from the California Institute of Technology (2003). After postdoctoral studies (also at Caltech), he became an assistant professor of chemistry at The University of Texas at Austin in 2004 and was promoted to associate professor in 2009, and professor in 2010. Prof. Bielawski's research program focuses primarily on synthetic problems at the interface of polymer, organic, and materials chemistry.

Rodney S. Ruoff is a Cockrell Family Regents Chair at The University of Texas at Austin, after having been Director of the Biologically Inspired Materials Institute and John Evans Chair at Northwestern University. He received his BS in Chemistry from UT-Austin and Ph.D. in Chemical Physics from the UI-Urbana (advisor H.S. Gutowsky). Prior to Northwestern he was a Staff Scientist at the Molecular Physics Laboratory of SRI International and Associate Professor of Physics at Washington University at St. Louis. He has 238 refereed journal articles in the fields of chemistry, physics, mechanics, and materials science, and is a co-founder of Graphene Energy Inc., and founder of Graphene Materials, LLC and Nanode, Inc.